Oblique collision in the northeastern Caribbean from GPS measurements and geological observations

Paul Mann,[1] Eric Calais,[2] Jean-Claude Ruegg,[3] Charles DeMets,[4] Pamela E. Jansma,[5] and Glen S. Mattioli[6]

Received 31 May 2001; revised 16 April 2002; accepted 10 June 2002; published 11 December 2002.

[1] Previous Caribbean GPS studies have shown that the rigid interior of the Caribbean plate is moving east-northeastward (070°) at a rate of 18–20 ± 3 mm/yr relative to North America. This direction implies maximum oblique convergence between the island of Hispaniola on the Caribbean plate and the 22–27-km-thick crust of the Bahama carbonate platform on the adjacent North America plate. We present a tectonic interpretation of a 15-site GPS network which spans the Hispaniola-Bahama oblique collision zone and includes stable plate interior sites on both the North America and Caribbean plates. Measurements span the time period of 1994–1999. In a North America reference frame, GPS velocities in Puerto Rico, St. Croix, and the Lesser Antilles indicate that these areas move as a single block in an east-northeast direction (070°) at a rate of 19–20 mm/yr consistent with the movement of the rigid interior of the Caribbean plate. GPS velocities at six sites in central and eastern Hispaniola (Dominican Republic) show drastically different behavior with more eastwardly strikes (080°) and much slower rates (4–17 mm/yr) than areas of the stable Caribbean plate. The boundary between the relatively slower-moving Hispaniola collisional zone and the relatively faster-moving, uncollided Puerto Rico-Virgin Islands area is the Mona Passage where late Neogene rifting occurs in a broad zone. Elastic modeling favors strain partitioning with oblique slip on the outer, low-angle submarine thrust faults (North Hispaniola, Muertos) and strike slip on the inner, subvertical subaerial, strike-slip faults (Septentrional, Enriquillo). *INDEX TERMS:* 8107 Tectonophysics: Continental neotectonics; 8105 Tectonophysics: Continental margins and sedimentary basins; 3025 Marine Geology and Geophysics: Marine seismics (0935); 3040 Marine Geology and Geophysics: Plate tectonics (8150, 8155, 8157, 8158); 7230 Seismology: Seismicity and seismotectonics; *KEYWORDS:* GPS, neotectonics, Hispaniola, Puerto Rico, Bahama Platform, earthquakes. **Citation:** Mann, P., E. Calais, J.-C. Ruegg, C. DeMets, P. E. Jansma, and G. S. Mattioli, Oblique collision in the northeastern Caribbean from GPS measurements and geological observations, *Tectonics*, *21*(6), 1057, doi:10.1029/2001TC001304, 2002.

1. Introduction

1.1. Neotectonics in the Northeastern Caribbean

[2] Prior to applications of GPS-based geodesy, the direction and rate of Caribbean plate motion remained controversial because the Caribbean plate is mainly bounded by subduction or strike-slip boundaries where plate rates and directions are difficult to precisely estimate from geologic structures and earthquakes alone (Figure 1a). For example, along the North America-Caribbean strike-slip boundary, measurements using fault strikes, and earthquake focal mechanisms had produced results varying in plate motion direction from due eastward at a rate of about 1–2 cm/yr [*Mann et al.*, 1991; *Calais and Mercier de Lépinay*, 1993; *DeMets et al.*, 1994] to east-northeastward at a rate of 4 cm/yr [*Sykes et al.*, 1982; *Deng and Sykes*, 1995]. Recent GPS measurements made at two islands, San Andres and Aves, that are well within the aseismic, stable interior of the Caribbean plate (Figure 1b), together with mapped fault strikes from the strike-slip segment of the North America-Caribbean plate, have demonstrated that the Caribbean plate is moving east-northeastward (070°) at a rate of 18–20 mm/yr relative to North America [*DeMets et al.*, 2000]. This rate is about 65% faster than the prediction of the Nuvel-1A global plate motion model of *DeMets et al.* [1994]. In addition, the direction implies maximum oblique plate convergence between the Caribbean and North America plates centered on the topographically elevated and seismogenic island of Hispaniola (Figure 1b).

[3] Plate boundary deformation and the long-term geologic evolution of the 600-km-long tectonic transition between westward subduction beneath the Lesser Antilles arc and strike-slip faulting in western Hispaniola has been intensively studied over the past 30 years using earthquakes, subaerial geologic, and structural mapping and submarine

[1]Institute for Geophysics, University of Texas at Austin, Austin, Texas, USA.
[2]Department of Earth and Atmospheric Sciences, Purdue University, West Lafayette, Indiana, USA.
[3]Laboratoire de Tectonique, CNRS-UMR 7578, Institut de Physique de Globe de Paris, Paris, France.
[4]Department of Geology and Geophysics, University of Wisconsin, Madison, Wisconsin, USA.
[5]Department of Geosciences, University of Arkansas, Fayetteville, Arkansas, USA.
[6]Department of Geology, University of Puerto Rico, Mayaguez, Puerto Rico.

0278-7407/02/2001TC001304$12.00

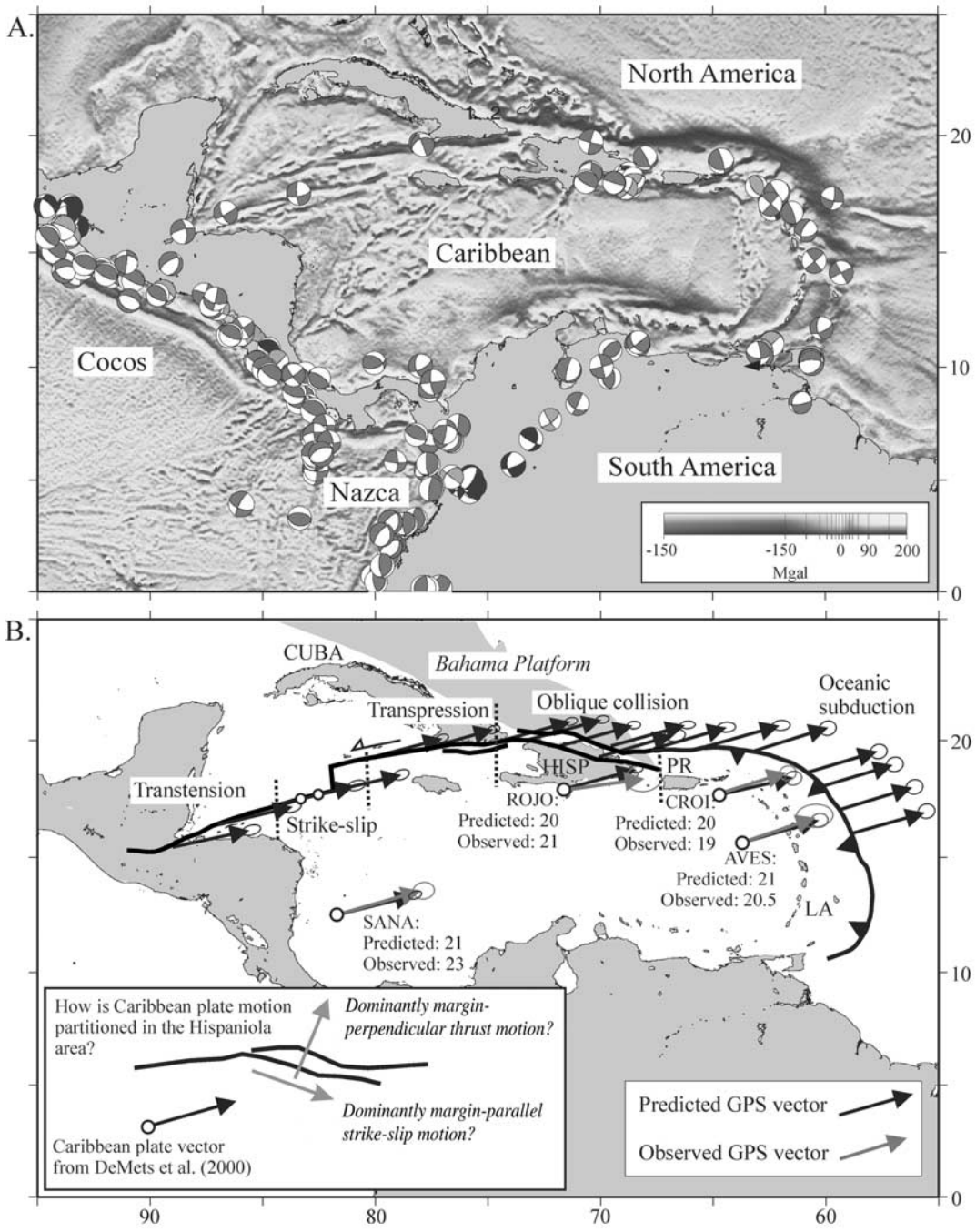

Figure 1. (a) Major plates of the Caribbean region and compilation of earthquake focal mechanisms showing present-day plate kinematics. Base map is a satellite-derived gravity map of the Caribbean compiled by *Sandwell and Smith* [1997]. Focal mechanisms shown in red are from earthquakes from 0 to 75 km in depth; blue mechanisms are from earthquakes 75 to 150 km in depth; and green mechanisms are >150 km in depth. (b) Caribbean-North America velocity predictions of *DeMets et al.* [2000] (black arrows) based on GPS velocities at four sites in the stable interior of the plate (red vectors) and two fault strike measurements in the strike-slip segment of the North America-Caribbean boundary (open circles). The predicted velocities are consistent with the along-strike transition in structural styles from transtension in the northwestern corner of the plate to oblique collision between the Caribbean plate in the Hispaniola (HISP) and Puerto Rico (PR) region and the Bahama Platform. One of the main objectives of this paper is to use GPS-based geodesy to determine how this motion is partitioned into margin-parallel strike-slip and margin-perpendicular thrust motions as shown in the inset diagram. See color version of this figure at back of this issue.

geophysical mapping (Figure 1a). These data types have led to varying conceptual models for neotectonics, strain partitioning, and microplates in the Hispaniola region that we reexamine in this paper using new GPS observations, elastic modeling, and recent geological and marine geophysical observations.

[4] In a complex plate boundary zone like Hispaniola, it is difficult to make direct comparisons between (1) geologic mapping data which record permanent deformation in Neogene rock structures; (2) GPS velocities recording interseismic elastic strain; and (3) earthquakes representing the sudden release of elastic strain. However, all three data types should in some way represent the continuation of progressive, late Neogene convergence between Hispaniola on the Caribbean plate and the Bahama Platform on the North America plate as predicted by plate tectonic reconstructions [e.g., *McCann and Sykes*, 1984; *Müller et al.*, 1999]. An integrated understanding of both the long-term pattern of permanent deformation and the present-day, interseismic elastic strain accumulation on active faults within the plate boundary zone constitutes a critical step in both understanding the tectonic development of the region and quantitative estimates of seismic hazard in Hispaniola, Puerto Rico, and the Virgin Islands that have a combined population of about 21 million people.

1.2. Previous Models for Hispaniola Neotectonics

[5] The first conceptual model emphasizes the dominance of late Neogene to recent strike-slip restraining bend convergence on the west-northwest trending and left-lateral Septentrional fault zone of northern Hispaniola and its combined left-lateral shear effect with the parallel and left-lateral Enriquillo fault zone of southern Hispaniola [*Mann et al.*, 1984; *Calais and Mercier de Lépinay*, 1993; *Russo and Villaseñor*, 1995] (Figure 2a). This model assumed that both strike-slip faults were relatively simple, vertical structures which accommodated all or most of the present-day North America-Caribbean strike-slip motion. Plate motion was assumed on the basis of widely accepted global plate motion models to be oriented in an east-west direction [*Jordan*, 1975; *DeMets et al.*, 1994; *Lundgren and Russo*, 1996]. *Dixon et al.* [1998] assumed this east-west strike-slip fault geometry for their 2-D elastic models of initial GPS results at five sites from Hispaniola.

[6] Later models for Hispaniola neotectonics emphasize the presence of low-angle subduction thrusts continuous with downdip Benioff zones bordering the northern (North Hispaniola fault zone-Puerto Rico trench) and southern (Muertos) margins of the island coexisting with onshore strike-slip faults (Figure 2b). The offshore thrusts were attributed to either more oblique west-southwestward convergence between North America and the Caribbean [*Deng and Sykes*, 1995], late Neogene north-south convergence between the North and South American plates [*Dillon et al.*, 1994; *Dixon and Mao*, 1997; *Müller et al.*, 1999], or progressive oblique collision between the southeastern Bahama Platform and Hispaniola [*McCann and Sykes*, 1984; *Mann et al.*, 1995; *Dolan et al.*, 1998].

1.3. Objectives of This Paper

[7] The central objective of this paper is to use new GPS-based geodetic results to test the three previous models for Hispaniola neotectonics. The Global Positioning System has largely proven to be well suited for measuring crustal deformation at plate boundary zones because of its high level of accuracy (2–3 mm horizontally over distances up to several hundreds of kilometers) and because large networks can be established and occupied at a modest cost. In this paper, we present the results of GPS measurements from 16 sites measured in the period 1994–1999 in Hispaniola, Puerto Rico, Virgin Islands, Lesser Antilles, Aves Island in the eastern Caribbean, and Barbados (Figure 3). The densest site distribution (10 sites) occurs on the eastern two thirds of the island of Hispaniola (Dominican Republic). This paper complements earlier GPS results in the northeastern Caribbean presented by (1) *Dixon et al.* [1998], based on five sites and measurements epochs covering the 1989–1995 period; (2) *Jansma et al.* [2000] focused on Puerto Rico and the Virgin Islands; and (3) *DeMets et al.* [2000] focused on the rigid kinematics of the Caribbean plate (Figure 1b).

[8] In this work, we add GPS observation epochs through 1999 and include new GPS sites in the analysis. We benefit from the improved North America-Caribbean GPS-based plate model of *DeMets et al.* [2000]; a wider field of observation allowed by the larger network area; and the improved geologic and marine geophysical mapping which has confirmed the coexistence of onland, late Holocene strike-slip zones flanked by offshore, low-angle thrust faults [e.g., *Dolan et al.*, 1998; *Mann et al.*, 1998] (Figure 2). We explore the implications of these newly studied faults for our GPS results and elastic models.

1.4. Significance of GPS Results

[9] Integration of previous geologic data, new GPS results, and elastic strain modeling in order to address three main questions which relate directly to the two different conceptual models for Hispaniola neotectonics discussed above and are relevant to the understanding of deformation is tectonically similar settings: (1) how is motion partitioned between strike-slip and thrust faults in Hispaniola?; (2) is Hispaniola currently behaving as a separate microplate detached by oblique convergence with the east-southeast trending promontory of the Bahama Platform on the North America plate?; and (3) what are the implications of Hispaniola-Bahamas convergence for seismic hazard assessment in the Hispaniola relative to adjacent plate boundary areas to the east in Puerto Rico, Virgin Islands, and northern Lesser Antilles?

1.5. Strain Partitioning

[10] The first question is how interplate motion between the North America and Caribbean plates is partitioned between margin-parallel strike-slip and margin-perpendicular thrust motions as shown schematically in the inset box of

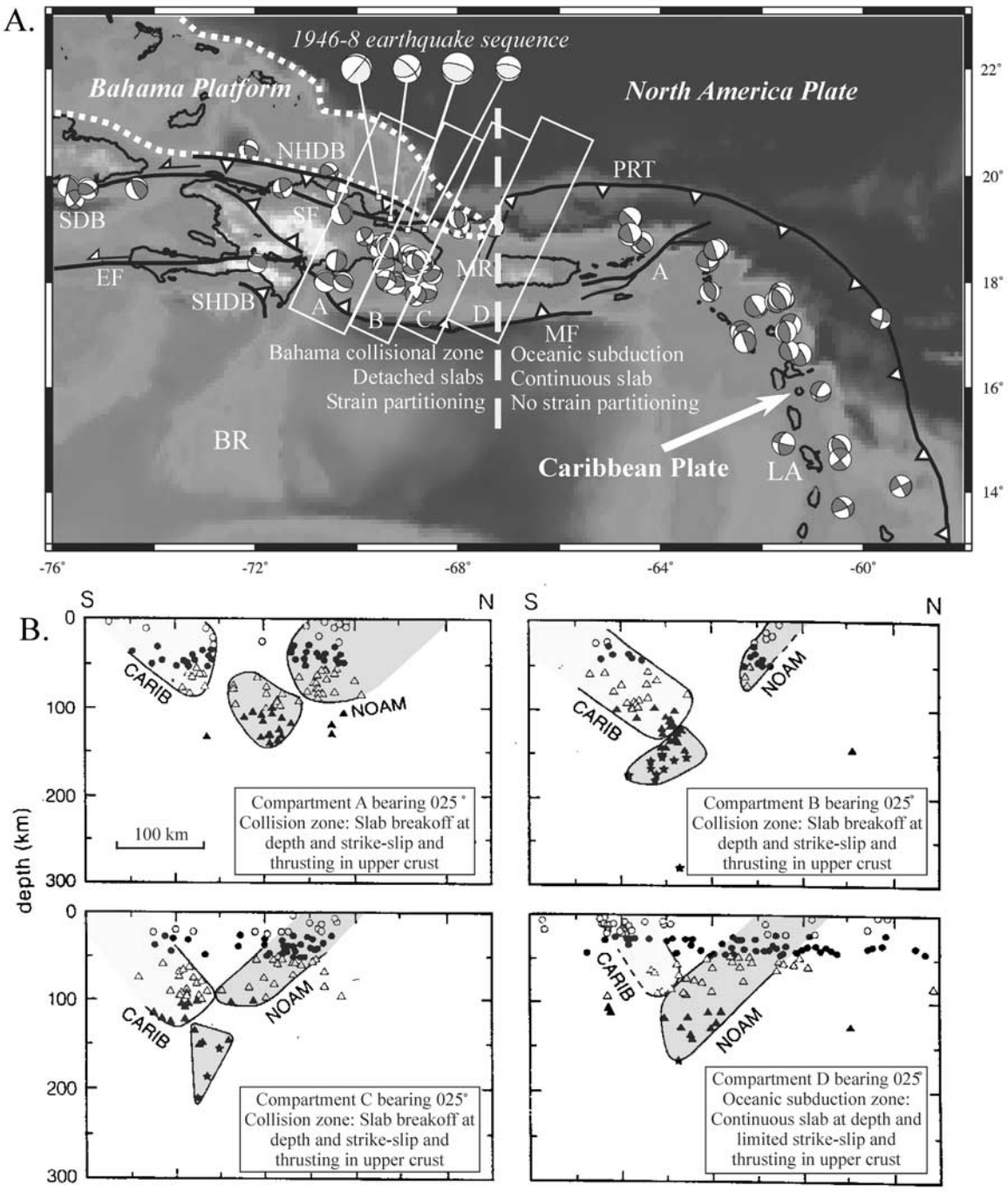

Figure 2. (a) Earthquake focal mechanisms along the northeastern margin of the Caribbean plate compared to the Caribbean-North America convergence direction. Focal mechanisms are from earthquakes from 0 to 50 km in depth: mechanisms in yellow are 1946-8 earthquake sequence [*Dolan and Wald*, 1998]; red mechanisms are compiled from the CMT catalogue [*Calais et al.*, 1992; *Molnar and Sykes*, 1969]. Most earthquake focal planes indicate thrusting along low-angle fault planes perpendicular to the *DeMets et al.* [2000] plate vector in the region of oceanic subduction east of the yellow, dashed line parallel to 67°W. West of this line, focal planes indicate strike-slip and oblique thrusting along variably oriented fault planes suggestive of strain partitioning within the Hispaniola-Bahama collision zone. (b) Plots of earthquake hypocenters in the Bahama Platform-Hispaniola-Puerto Rico collisional zone projected to planes passing through each of the compartments shown on the map in A (modified from *Dillon et al.* [1994]). Inferred tectonic setting, slab geometry, and crustal deformational style of each compartment is summarized in inset. See color version of this figure at back of this issue.

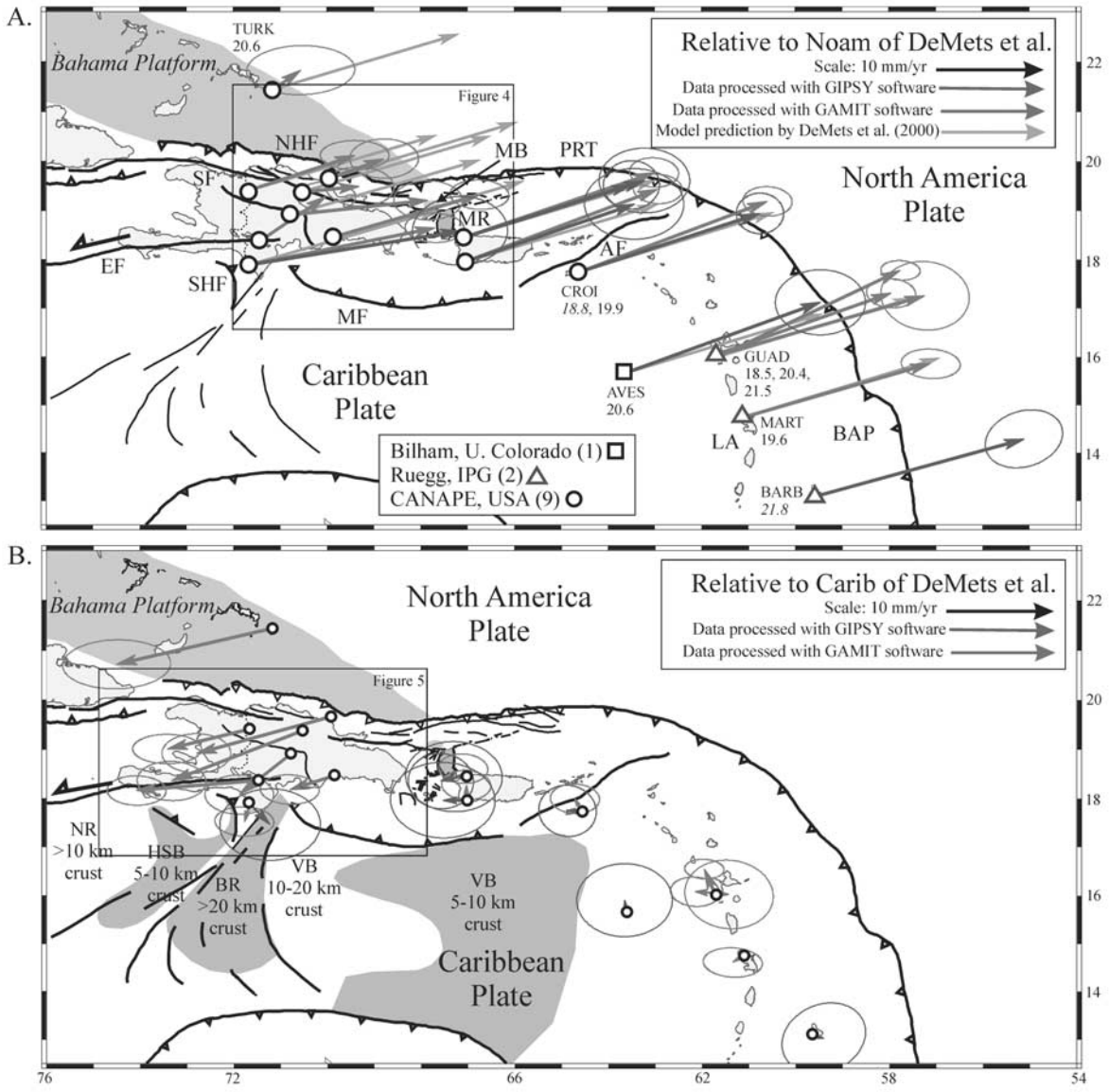

Figure 3. (a) Comparison of observed GPS velocities for Caribbean sites relative to North America. Color code for velocities shown in inset. Abbreviations for GPS sites: BARB, Barbados; MART, Martinique; GUAD, Guadeloupe; AVES, Aves Island; CRO1, St. Croix, U.S. Virgin Islands; TURK, Turk Island, Bahamas. Abbreviations of tectonic features: BAP, Barbados accretionary prism; LA, Lesser Antilles volcanic arc; AF, Anegada fault; PRT, Puerto Rico trench; MR, Mona rift (gray area); MF, Muertos fault; MB, Mona block; NHF, North Hispaniola fault; EF, Enriquillo fault; SHF, South Haiti fault. (b) Comparison of observed GPS velocities relative to the stable Caribbean plate as defined by *DeMets et al.* [2000]. Velocities show a strong southwestward component consistent with southwestward thrusting of late Miocene to recent age in Hispaniola. Variations in the crustal thickness of the Caribbean oceanic plateau on the Caribbean plate as determined by *Mauffret and Leroy* [1997] are shown. Abbreviations: NR, Nicaraguan Rise; HSB, Haiti subbasin; BR, Beata Ridge; VB, Venezuelan basin. See color version of this figure at back of this issue.

Figure 1b. This question is fundamentally important for understanding the mechanics of obliquely convergent active margins [*McCaffrey*, 1992]. The question of strain partitioning is also critical for understanding the types and locations of future earthquakes in this densely populated sector of the plate boundary zone. For present-day estimates of strain partitioning into margin-parallel and margin-perpendicular components, we rely on 3-D elastic models constrained by GPS results and fault slip rates and fault dips taken from previous geologic studies and reviewed in maps and cross

sections presented in this paper. *DeMets et al.* [2000] note that the plate-normal component of Caribbean-North America motion the 650-km-long segment of the Hispaniola restraining bend is 2 to 5 times higher (up to 11 ± 3 mm/yr) than that predicted by their plate model for other areas along the ~3000-km-long plate boundary.

1.6. Microplates

[11] The second question on the existence of microplates in Hispaniola is addressed by study of GPS velocities in the area of the proposed Hispaniola-Puerto Rico microplate of *Byrne et al.* [1985] in eastern Hispaniola and the Mona Passage and the proposed Gonave microplate of *Mann et al.* [1995] in the area of central and western Hispaniola. A recent GPS study by *Jansma et al.* [2000] revealed that the Puerto Rico-northern Virgin Islands microplate proposed by *Masson and Scanlon* [1991] on the basis of marine geophysical data is moving at a rate no faster than about 1 mm/yr relative to the stable Caribbean plate. Longer time series at sites which were not available for the *Jansma et al.* [2000] or this paper will better address the problem of whether any slow (<1 mm/yr) relative motion exists between Puerto Rico and the rest of the Caribbean plate. *Jansma et al.* [2000] showed that GPS data from Puerto Rico and Hispaniola is consistent with about 5 mm/yr of opening in the Mona Passage, the marine strait between the two islands. The presence of microplates and their boundaries with the Caribbean and North American plate is an important question both for the long-term geologic evolution of the area and the associated seismic hazards of these boundaries.

1.7. Seismic Hazards

[12] A third and final set of questions relates to the seismic hazard of this particularly wide, seismogenic, and densely populated segment of the North America-Caribbean plate boundary where geologic fault slip studies have only been conducted on only one segment of the Septentrional fault [*Prentice et al.*, 1993; *Mann et al.*, 1998; *Prentice et al.*, 2002] (Figure 2a) and where numerous, large historical earthquakes felt over the past 500 years may have originated on the inner set of strike-slip faults (Septentrional, Enriquillo) or on the outer set of low-angle thrust faults (North Hispaniola-Puerto Rico). These historical events are potentially large and destructive as shown by the M7.2–8.1 1943–1953 earthquake series that occurred along the low-angle North Hispaniola fault between northeastern Hispaniola and the Bahama Platform [*Dolan and Wald*, 1998] (Figure 2a). We use GPS data to constrain fault slip rates and elastic strain accumulation across various segments of the plate boundary and derive information on earthquake potential.

2. GPS Data and Processing

2.1. Data Distribution and Acquisition

[13] In order to address these problems, we have combined GPS data sets collected by collaborating U.S. and French institutions in Hispaniola, the Bahama Platform, and the Lesser Antilles. GPS measurements were first carried out in the northeastern Caribbean in 1986 at a total of six sites on the Bahamas Platform (TURK), southern Cuba (GTMO), St. Croix, U.S. Virgin Islands (SCRX) and three sites in Hispaniola (ROJO, FRAN, CAPO [*Dixon et al.*, 1991]) (Figures 1 and 3).

Table 1. Observation Schedule of the GPS Campaign Sites in the Northeastern Caribbean Presented in This Study

				Observation Epochs						
Number	Code	Full Name		86	94	95	96	97	98	99
1	CAPO	Capotillo JPL	DR	x	x				x	
2	CONS	Constanza	DR		x				x	
3	FRAN	Cabo Frances Viejo	DR	x	x				x	
4	MOCA	Moca	DR		x				x	
5	ROJO	Cabo Rojo	DR	x	x				x	
6	SDOM	Santo Domingo	DR		x				x	
7	COLO	La Colonia	DR		x				x	
8	ISAB	La Isabella	PR	x	x	x	x		x	
9	PARG	Parguera	PR		x		x	x	x	
10	CRO1	St Croix	VI			x	x	x	x	x
11	AVES	Aves island	Vene.		x				x	
12	TURK	Grand Turk	Bah.	x	x				x	
13	MAT0	Matouba	Guad.			x			x	
14	RCB1	Chutes du Carbet	Guad.			x			x	
15	HOU0	Houelmont	Guad.		x	x			x	
16	FSD0	Fonds St Denis	Mart.		x		x		x	

[14] These sites were reoccupied in 1994 and the network was densified in 1998 to include an additional 15 sites in the Dominican Republic, Puerto Rico, and the Virgin Islands as part of the U.S.-French CANAPE project (Caribbean North America Plate Experiment) [*Dixon et al.*, 1998]. Partial remeasurements of the network were subsequently carried out in 1995, 1996, 1997, and 1999. In this study, we use these data along with GPS data from permanent sites at St. Croix (CRO1) and Barbados (BARB) which have operated in the framework of the International GPS Service for Geodynamics (IGS) since October 1995, and November 1997, respectively (Table 1).

[15] We also integrated GPS data collected at four sites in Martinique and Guadeloupe in the Lesser Antilles by the Institut de Physique du Globe de Paris, and one occupation [1994] at Aves Island by the University of Colorado at Boulder (data courtesy of R. Bilham) (Figure 3). The GPS results presented here are therefore based on a network of 16 sites, seven in the Dominican Republic in Hispaniola, two in Puerto Rico, and one in St. Croix (US Virgin Islands), one on Aves Island, and five in the Lesser Antilles (Table 1). The entire GPS data set spans an area of about 1600 by 850 km or about 30% of the entire area of the Caribbean plate (Figure 1). This regional scale of observation is particularly important for addressing the question of microplate tectonics along the northern Caribbean plate boundary zone.

[16] GPS campaign data were collected using various dual-frequency, code phase receiver/antenna combinations. The 1994 measurements were performed using Ashtech Z12 receivers with Geodetic II antennae and Trimble 4000 SSE with Trimble SST antennae. In 1996, we used Trimble 4000 SSE with Trimble SST antennae. All observations after June

Table 2. GPS Horizontal Stations Positions, Velocities, and Associated Formal Errors[a]

			ITRF97					NOAM		CARB	
Site	Lon.	Lat.	Ve	Vn	σve	σvn	Corr.	Ve	Vn	Ve	Vn
CAPO	−71.67	19.42	2.20	6.00	0.70	0.30	−0.0080	10.55	3.49	−8.21	−2.00
COLO	−71.45	18.37	−1.30	7.10	0.60	0.30	−0.0225	6.68	4.51	−12.27	−1.00
CONS	−70.77	18.92	5.50	4.30	0.70	0.40	−0.0146	13.66	1.45	−5.21	−4.10
RCB1	−61.65	16.04	13.70	12.20	0.90	0.70	−0.0608	20.64	5.92	1.05	−0.06
MAT0	−61.69	16.05	10.50	12.40	0.50	0.30	−0.0754	17.44	6.13	−2.15	0.16
HOU0	−61.70	15.98	11.50	15.00	0.40	0.20	−0.0716	18.42	8.74	−1.18	2.76
FSD0	−61.15	14.73	12.40	11.90	0.60	0.30	−0.0808	18.87	5.43	−0.91	−0.56
FRAN	−69.94	19.67	−3.00	5.10	0.70	0.40	0.0024	5.41	1.93	−13.36	−3.66
ISAB	−67.05	18.47	10.90	10.70	0.50	0.30	−0.0647	18.83	6.43	−0.24	0.70
MOCA	−70.53	19.38	−2.60	3.50	0.70	0.40	−0.0390	5.72	0.56	−13.08	−5.00
PARA	−67.04	17.97	11.40	11.50	0.50	0.30	−0.0573	19.15	7.23	0.01	1.49
ROJO	−71.67	17.90	10.70	6.20	0.60	0.30	−0.0496	18.51	3.69	−0.50	−1.80
SDOM	−69.87	18.47	6.60	7.40	0.60	0.30	−0.0535	14.59	4.21	−4.39	−1.39
TURK	−71.13	21.46	−6.40	4.60	1.10	0.50	0.0378	2.65	1.89	−15.76	−3.64
CRO1	−64.58	17.76	11.00	12.20	0.50	0.30	−0.0474	18.62	7.01	−0.64	1.16

[a]Velocities are given in mm/yr. Formal errors (σv) are in mm, one standard deviation. Abbreviations are as follows: ITRF97, International Terrestrial Reference Frame 1997 [*Boucher et al.*, 1999]; NOAM, North American plate; CARB, Caribbean plate. Abbreviations are as follows: Lon, longitude; Lat, latitude; Ve and Vn, east and north velocity components; Corr, correspondence.

1996, with the exception of the 1998 campaigns at San Andres Island (SANA) and Aves Island (AVES), were obtained with Trimble 4000 SSI with Dorne-Margolin choke-ring antennae. Each site was surveyed 22 to 24 hours a day for an average of three consecutive days during each campaign. The data were collected at a 30 s sampling rate using a 10° elevation cutoff angle.

2.2. Data Processing

[17] We processed pseudorange and phase GPS data in single-day solutions using the GAMIT software. We solved for regional station coordinates, satellite state vectors, 13 tropospheric zenith delay parameters per site and day, and phase ambiguities using doubly differenced GPS phase measurements. We used IGS final orbits, IERS (International Earth Rotation Service) earth orientation parameters, and applied azimuth and elevation dependant antenna phase center models, following the tables recommended by the IGS. We included 11 global IGS stations with position and velocities well determined in the International Terrestrial Reference Frame (ITRF97) [*Boucher et al.*, 1999] to serve as ties with the global reference frame (stations GOLD, BRMU, ALGO, CRO1, KOUR, MAS1, RSM5, RCM6, AREQ, SANT, KOKB).

[18] The least squares adjustment vector and its corresponding variance-covariance matrix for station positions and orbital elements estimated for each independent daily solution were then merged together using a Kalman filter. We also added daily solutions from global tracking sites obtained from the IGS data processing center at Scripps Institution of Oceanography. Site positions and velocities, earth orientation parameters, and orbits were loosely constrained at this stage.

[19] We then impose the reference frame using the resulting combined solution by minimizing the position and velocity deviations of 14 IGS stations with respect to the ITRF97, while estimating an orientation, translation and scale transformation. The height coordinate and velocity were downweighted by a factor of 10 relative to the horizontal components.

2.3. Site Velocities and Errors

[20] Our results over the 5 year period 1994–1999 are listed in Table 2. We assess the accuracy of the GPS estimates using daily and long-term baseline repeatabilities based on weighted RMS scatter about the best fit linear regression to the position time series. We find long-term baseline repeatabilities of the order of 2–4 mm for the horizontal components and 5 to 10 mm for the vertical component.

[21] The formal errors of the GPS-derived velocities have been computed by scaling the 1-σ uncertainties of the final adjustment by the overall chi-square per degree of freedom. The formal standard deviations are typically of the order of 2 mm/yr and 4 mm/yr for the north and east velocity components, respectively, assuming a pure white noise error model for site positions [*Mao et al.*, 1999]. Time series analysis of continuous position time series in California and at global sites [*Mao et al.*, 1999] have shown that GPS position estimates follow a noise model that combines white and colored noise. If similar noise spectra apply to our station positions, the actual uncertainties could be 2–4 times larger than those derived from a white noise model only. Velocity vectors shown in the figures are represented with their two-dimensional 95% confidence limit.

2.4. Local and Regional Reference Frames

[22] Tectonic interpretation of geodetic results requires a representation of the velocity field with respect to a rigid block such as a plate interior. This is usually done by removing a rigid plate rotation taken from a global kinematic model or estimated from the velocities at a number of geodetic sites on that plate. Using 16 permanent GPS stations in the stable interior of the North American plate, *DeMets and Dixon* [1999] estimated rotation parameters for

Table 3. Caribbean (CARIB) and North American (NOAM) Plate Angular Velocities and Uncertainties[a]

	Latitude, °N	Longitude, °E	Rotation Rate, °/Myr	Major Axis	Minor Axis	Azimuth Clockwise	Uncertainty in Rotation Rate
NOAM/ITRF97	−3.1	281.8	0.199	1.5	0.5	−12	0.003
CARIB/ITRF97	36.9	270.7	0.297	4.8	1.1	−22	0.033
CARIB-NOAM	73.1	228.9	0.198	13.6	1.6	−56	0.017

[a]In each case, the first plate rotates CCW about the pole with respect to the fixed frame. ITRF97 stands for Interntational Terrestrial Reference Frame-1997.

the North American plate with respect to the ITRF96. Similarly, *DeMets et al.* [2000] estimated rotation parameters for the Caribbean plate relative to ITRF96 using four GPS sites on the Caribbean plate interior and two azimuths of the Swan Islands transform fault along the southern edge of the Cayman trough [*Rosencrantz and Mann*, 1991] (Figure 1b). In this study, we reestimate the angular velocities of the Caribbean and North American plates employing updated GPS velocities for Caribbean and North American plate sites and the most recent geodetic reference frame ITRF97 [*Boucher et al.*, 1999]. The NOAM-ITRF97 and CARB-ITRF97 rotation parameters are given in Table 3.

[23] For the Caribbean plate, we use two azimuths from the Swan Islands transform fault and the velocities of our GPS sites (SANA, AVES, ROJO, and CRO1) (Figure 1b). The GPS sites incorporate all data available as of August 2000. The residual velocities at these sites average 1.3 mm/yr for both the north and east components. For the North American plate, we used velocities from 100 sites that have operated continuously for periods ranging from 2.0 to 7.2 years. Although the geographic extent of these sites is no greater than for the 16 sites employed by *DeMets and Dixon* [1999] to estimate the North American plate angular velocity, increases in both the length of the GPS time series and the number of sites we employ reduce the uncertainties in the North American angular velocity to negligible levels (Table 3). The residual velocities at these sites average 1.0 mm/yr in both the north and east components.

[24] To represent our results in a North America frame, we therefore rotated our ITRF97 velocities by differentiating the measured and predicted North America-ITRF97 velocity at each of our GPS sites (Figure 3a). Similarly, we represent our results in a Caribbean frame (Figure 3b) by differentiating the measured and predicted Caribbean-ITRF97 velocity at each of our GPS sites.

3. GPS Results and Elastic Strain Models

3.1. GPS Observations

[25] Figures 3a and 3b display the GPS-derived velocities in North American and Caribbean fixed reference frames, respectively. In a North America fixed frame, we find an insignificant residual velocity of 3.3 ± 3.3 mm/yr at site TURK on the Bahamas platform, consistent with the previous interpretation of *Dixon et al.* [1998] that this site is located on the stable North America plate.

[26] For the sites located in Puerto Rico (ISAB, PARA), St. Croix (CRO1), Guadeloupe (GUAD), Martinique (MART), Aves Island, (AVES), and Barbados (BARB), we find GPS velocities in very good agreement with *DeMets et al.*'s [2000] kinematic model predictions for the Caribbean plate (Figure 1b). Residual velocities at these sites (see velocities in a Caribbean fixed frame, Figure 5) range from 0.6 mm/yr to 3.3 mm/yr (1.4 mm/yr on average) and are insignificant at the 95% confidence level. The same is true for ROJO, located at the southernmost tip of Hispaniola (Figure 4a). Its velocity is consistent with the prediction of a rigid Caribbean model, with a residual velocity of 1.9 mm/yr (Figure 3b).

Figure 4. (opposite) (a) Crustal tectonic features of the Hispaniola-Bahama collision zone in Hispaniola (HISP, includes Dominican Republic and Haiti) compared with GPS velocities relative to the North America. Abbreviations for GPS sites: PARG, Parguera, Puerto Rico; ISAB, La Isabela, P.R.; SDOM, Santo Domingo, Dominican Republic; ROJO, Cabo Rojo, D.R.; COLO, Colorado, D.R.; CONS, Constanza, D.R.; CAPO, Capotillo, D.R.; MOCA, Moca, D.R.; FRAN, Cabo Frances Viejo, D.R. The velocities straddle the boundary of the Hispaniola-Bahama collisional zone, whose eastern limit is defined by the subducted carbonate high of the Bahama Platform, the Mona Block (MB), and the adjacent Mona rift (MR). The now-subducted Mona block is collinear with presumably similar carbonate highs to the northwest: the Navidad (NB), Silver (SB), and Mouchoir (MB) Banks. These banks grew to sea level on top of a broad, Mesozoic carbonate "megaplatform" now at an average depth of 4000 m. Active tectonic features of the overriding plate include thrust faults of the North Hispaniola fault (NHF) and Puerto Rico trench (PRT), the North Puerto Rico Slope (NPRSF), the South Puerto Rico Slope (SPRSF), the Septentrional (SF) and the Enriquillo (EF) left-lateral strike-slip faults, the Puerto Rico-Virgin Islands (PRVI) arch, the Mona rift, and the Muertos fault (MF). (b) Subcrustal tectonic features of the Hispaniola-Bahamas collision zone include three areas of the subducted North America slab reproduced from *Dillon et al.* [1994]: an area of a continuous subducted slab in the east; an area of detached slab in the center; and an area to the west where no slab has been mapped. The 1943–1953 earthquakes (stars) and their magnitudes are in the general area of the continuous subducted slab and probably represent increased coupling between the carbonate banks on the downgoing plate and the overriding Caribbean plate in Hispaniola. See color version of this figure at back of this issue.

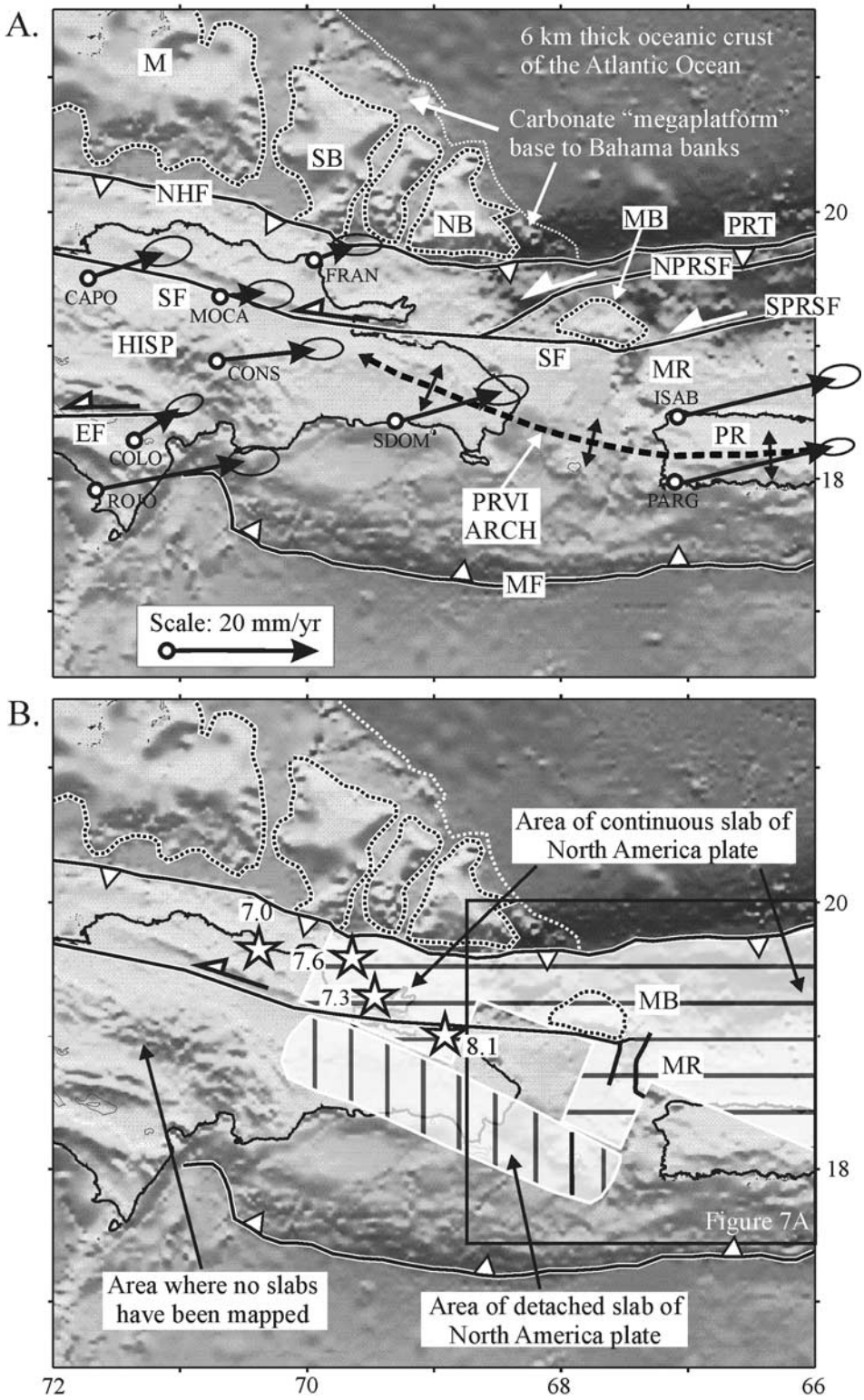
A.
6 km thick oceanic crust of the Atlantic Ocean
Carbonate "megaplatform" base to Bahama banks
M
SB
NHF
NB
MB
PRT
NPRSF
SPRSF
CAPO
SF
MOCA
FRAN
HISP
CONS
SF
MR
ISAB
EF
COLO
SDOM
PR
ROJO
PRVI ARCH
PARG
MF
Scale: 20 mm/yr
20
18
B.
Area of continuous slab of North America plate
7.0
7.6
7.3
8.1
MB
MR
20
18
Figure 7A
Area where no slabs have been mapped
Area of detached slab of North America plate
72
70
68
66

[27] GPS-derived velocities at five sites in central and eastern Hispaniola (CAPO, FRAN, CONS, MOCA, SDOM) show significant discrepancies with the prediction of a rigid Caribbean plate model as seen in the global, North America (Figure 3a), and Caribbean reference frames (Figure 3b). These sites have consistently more easterly strikes and slower rates than the sites in Puerto Rico, the Virgin Islands, and the Lesser Antilles that are moving as part of the stable Caribbean plate [*Jansma et al.*, 2000]. Residual velocities in a Caribbean fixed frame illustrate this result with residual velocities of 5–14 mm/yr in a west–southwest direction. In addition, one can observe a decrease in velocities from south to north across Hispaniola in the North America (Figure 3a) and Caribbean (Figure 3b) reference frames.

[28] This spatial gradient, perpendicular to the trend of the roughly east–west trending plate boundary zone, could be caused by either elastic strain accumulation on individual locked faults in Hispaniola shown in Figure 2a or continuous and/or anelastic deformation across the entire Hispaniola plate boundary zone. However, four, throughgoing active faults, mapped onland and offshore and spatially associated with large historical earthquakes, appear to concentrate interplate strain in Hispaniola. We show the locations of these faults in Figures 4 and 5 including their relationships to (1) surface topography; (2) GPS velocities in both a North American and Caribbean frame; (3) the epicenters of large historical earthquakes; and (5) subducted slabs known from earthquake studies.

3.2. Major Active Faults in Hispaniola

3.2.1. Onland Strike-Slip Faults

[29] The maps of Figures 4 and 5 show the two main left-lateral strike-slip faults in Hispaniola, the Septentrional and Enriquillo faults. In northern Hispaniola, the right stepping, left-lateral Septentrional fault is responsible for the uplift of the Cordillera Septentrional in its area of maximum fault curvature in the northern Dominican Republic and for active folding and faulting at its contact with late Neogene to Holocene units of the Cibao valley [*Calais et al.*, 1992; *Mann et al.*, 1998]. Fault trenching studies by *Prentice et al.* [1993], *Mann et al.* [1998], and *Prentice et al.* [2002] along the Septentrional fault in northern Dominican Republic show that the most recent ground-rupturing earthquake occurred over 800 years ago and involved a minimum of 4 m of left-lateral slip. In addition, offset stream terrace risers along the Septentrional fault provide Holocene left-lateral slip rate estimates of 9 ± 3 mm/yr [*Prentice et al.*, 2002]. Marine geophysical surveys north of Hispaniola [*Dillon et al.*, 1992; *Dolan et al.*, 1998] and Puerto Rico [*Masson and Scanlon*, 1991; *Grindlay et al.*, 1997] indicate that the Septentrional fault zone extends eastward as far as the Mona rift with earthquake evidence for strike-slip motion [*McCann and Sykes*, 1984; *Calais et al.*, 1992] (Figure 4a). The Septentrional fault extends westward along the northern coast of Haiti and along the southern Cuban margin [*Calais and Mercier de Lépinay*, 1991, 1993] (Figure 5a). In offshore areas, the fault appears vertical on seismic reflection profiles. In northern Hispaniola, seismic reflection profiles by *Edgar* [1991] reveal a complex, subvertical flower zone structure in rocks and sediments of late Neogene to Quaternary age.

[30] The east-west striking Enriquillo fault of southern Hispaniola is less well exposed because its trace lies in the Enriquillo Valley, a subsea level depression characterized by rapid alluvial fan and lake sedimentation along steep-sided mountain fronts (Figure 5a). Nevertheless, its location has been mapped locally at the surface and in the subsurface using seismic reflection data [*Mann et al.*, 1995, 1999]. The Enriquillo fault ends abruptly in south central Hispaniola and cannot be traced as a continuous east-west fault into eastern Hispaniola. Its possible that strike-slip motion along the Enriquillo fault is transferred southeastward to the active, low-angle thrust motion at the western terminus of the Muertos fault [*Mauffret and Leroy*, 1999] (Figure 5a). Motion on the low-angle Muertos thrust fault decreases from this point eastward to longitude 66°W where little or no active underthrusting is occurring [*Masson and Scanlon*, 1991]. The Enriquillo fault extends westward across the southern peninsula of Haiti and is continuous with the Plantain Garden fault zone of Jamaica [*Mann et al.*, 1995]. A number of historical earthquakes affected towns of southern Hispaniola in the 17th, 18th, and 19th centuries suggesting that they may have occurred on a major fault in southern Dominican Republic, possibly the Enriquillo fault (Figure 5a). However, no geological estimate of slip rate is yet available for this fault.

3.2.2. Offshore Oblique-Slip Faults and Subducted Slabs

[31] The North Hispaniola fault has been mapped using side scan sonar and seismic reflection data by *Dillon et al.* [1992] and *Dolan et al.* [1998] along the northern margin of the island (Figure 4a). These data suggest a very low-angle thrust boundary consistent with the occurrence of a series of M7.2–8.1 large thrust earthquakes in the period 1943–1953 [*Dolan and Wald*, 1998] (Figure 4b). The North Hispaniola fault is continuous with the Puerto Rico trench to the east which is the site of recent strike-slip and low-angle thrust faulting and a very strong (−400 mGal) negative gravity anomaly (Figure 1a). Both the North Hispaniola and Puerto Rico trench faults mark the site of subduction for slabs of Atlantic lithosphere beneath Hispaniola and Puerto Rico, respectively (Figure 2b). Detailed studies of earthquakes by *Dillon et al.* [1994] shows the presence of one or more slab fragments in the depth range of 70–200 km (Figure 2b). The slabs generally exhibit southward dips and therefore appear to be broken off from the southward or southwestward subducting North America plate. A boundary can be drawn near the west coast of Puerto Rico separating a continuous and unbroken subducted slab of Atlantic oceanic crust (North America plate) beneath the northern Lesser Antilles, the Virgin Islands, and Puerto Rico, and an area of detached slab(s) beneath the Mona Passage and eastern Hispaniola (Figure 2a).

3.3. Elastic Strain Model Assumptions

[32] We use the a priori and admittedly incomplete geologic information on active structures in the Hispaniola-

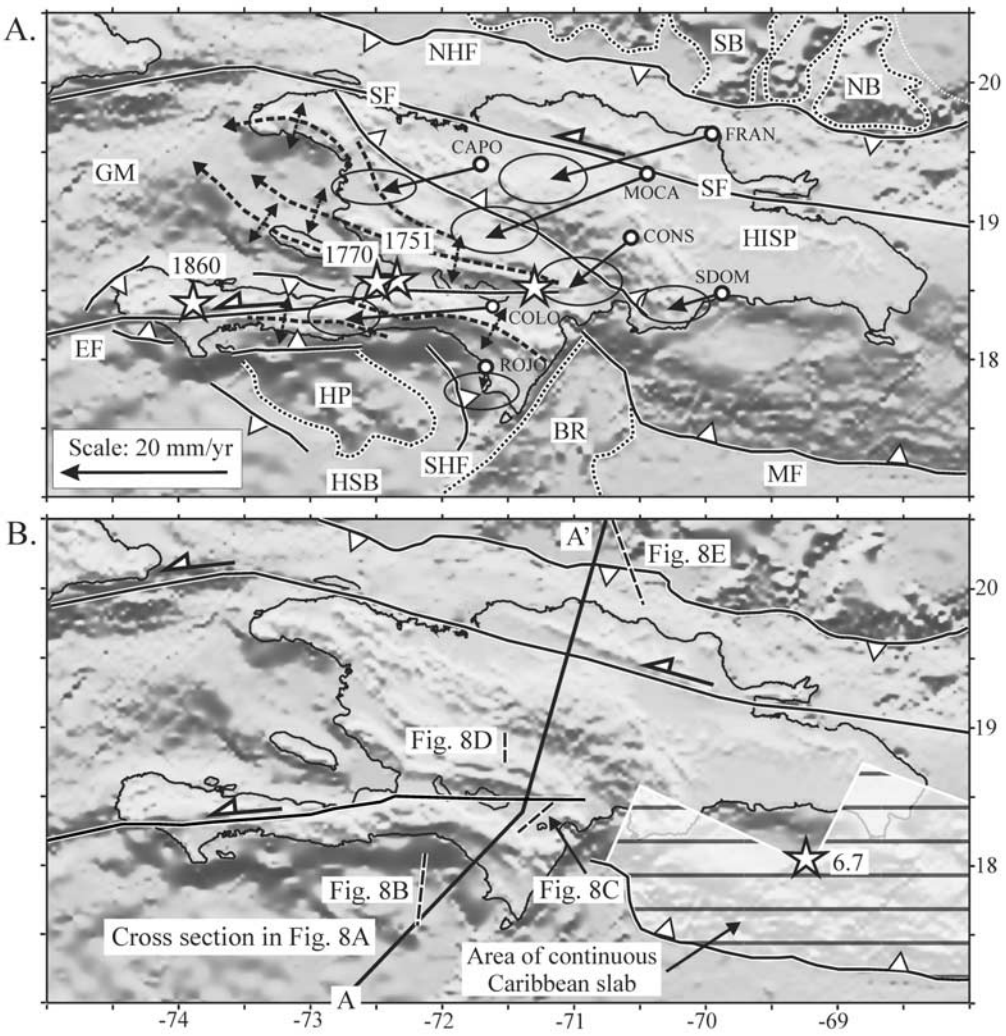

Figure 5. (a) Crustal tectonic features of the Hispaniola-Bahama collision zone compared with GPS velocities relative to the Caribbean plate reference frame. The velocities provide good across-strike coverage of the fold-thrust belt structure of Hispaniola (HISP) which represents southwestward backthrusting produced by the oblique collision of Hispaniola with the Bahama Platform. Stars represent a time-space progression of large historical earthquakes spatially associated with the Enriquillo fault that began in 1751 and extended westward to 1860. Abbreviations: SB, Silver Bank; NB, Navidad Bank; NHF, North Hispaniola fault; SF, Septentrional fault; EF, Enriquillo fault; SHF, South Haiti fault; BR, Beata Ridge; MT, Muertos fault; HP, Haiti Plateau; HSB, Haiti subbasin; GM, Gonave microplate. B. Subcrustal tectonic features of the Hispaniola-Bahama collision zone include an area of subducted Caribbean slab reproduced from *Dillon et al.* [1994]. The 1984 M6.7 thrust event occurred at a depth of 32 km and confirmed northward thrusting of the Caribbean plate beneath southeastern Hispaniola. See color version of this figure at back of this issue.

Puerto Rico area to construct a simple deformation model that assumes elastic strain accumulation on locked faults [e.g., *Savage*, 1983, 1990]. This deformation model uses GPS-derived velocities in order to gain a better understanding of the slip distribution on active faults across the plate boundary zone in Hispaniola. In particular, we are interested in distinguishing the previously discussed neotectonic model for a restraining bend on an east–west strike-slip fault from other models including simple oblique convergence without the influence of the Bahama Platform and localized oblique collision of the Bahama carbonate platform with Hispaniola. We are also interested in how the total Caribbean-North America plate convergence is partitioned into a margin-parallel (strike-slip) and margin-perpendicular (thrust) component of displacement as shown schematically in the inset of Figure 1b. Model-derived predictions for fault slip rates and fault character are necessary since only one fault in Hispaniola (the Septen-

trional) has geologic slip rate information derived from fault trenching.

[33] In an earlier paper, *Dixon et al.* [1998] modeled elastic strain accumulation along a two-dimensional north-south profile across the Dominican Republic. Their model was constrained by four GPS velocities and used assumptions of vertical strike-slip faults only because at the time of the study the GPS data was not sufficient to constrain fault-perpendicular motion. In this study, we use the more robust GPS data set shown in Figures 3, 4, and 5 to model elastic strain in three dimensions and use a larger number of GPS sites spanning central and eastern Hispaniola in the Dominican Republic and Puerto Rico. We also consider the low-angle nature of the North Hispaniola-Puerto Rico trench fault and the Muertos fault based on marine geophysical mapping.

[34] We model elastic strain in an elastic half-space cut by active faults assumed to be fully locked to shallow depth and freely slipping below that depth [*Feigl and Dupré*, 1999]. Following *Pollitz and Dixon* [1998], we assume that postseismic relaxation effects of the larger thrust events of the 1943–1953 earthquake series do not significantly contribute to surface crustal velocities in our network in the 1994–1999 time period.

[35] Input into the model includes fault location, dip, strike, and sense of slip constrained by geologic data compiled in Figures 4 and 5. Input into the elastic strain model also include fault-locking depth. Seismological studies indicate that most hypocenter of shallow (<30 km) earthquakes in the northeastern Caribbean area are located near 15 km [*Sykes et al.*, 1982; *Calais and Mercier de Lépinay*, 1991; *Deng and Sykes*, 1995; *Dolan et al.*, 1998], consistent with a continental or transitional crust of normal heat flow. In the absence of more detailed information, we assume in this model that all faults have a 15 km locking depth.

3.4. Test of Previously Published Fault Slip Rates

[36] We first test the fault slip rates proposed by two deformation models that have assumed that roughly east–west interplate strike-slip motion occurs along vertical strike-slip faults [*Lundgren and Russo*, 1996; *Dixon et al.*, 1998]. *Lundgren and Russo* [1996] tested the role of boundary conditions on interplate deformation in the northeastern Caribbean using an elastic, two-dimensional, spherical shell, finite element model that includes faults. Their best fit model predicts 4–8 mm/yr of left-lateral strike slip motion on the North Hispaniola fault, increasing from west to east; 10 mm/yr of left-lateral strike slip motion on the Septentrional fault, decreasing to 7–3 mm eastward along its eastward offshore prolongation; 1–3 mm/yr of left-lateral strike slip on the Enriquillo fault; 6–1 mm/yr of thrust motion across the Muertos fault, decreasing from west to east (Figure 6a and Tables 4 and 5).

[37] Using a subset of the GPS data used herein, principally the components of four GPS velocities from Hispaniola projected onto the local direction of the Septentrional fault (110°), *Dixon et al.* [1998] modeled the plate boundary parallel elastic strain accumulation in two dimensions along a profile across Hispaniola. Their best fit model predicts 4 ± 3 mm/yr of left-lateral slip on the North Hispaniola fault, 8 ± 3mm/yr on the Septentrional fault, and 8 ± 4 mm/yr on the Enriquillo fault (Figure 6b and Table 4). Although the GPS data were not sufficient to model the plate boundary-normal component, *Dixon et al.* [1998] estimated this component to be ~7 mm/yr. Projection of the GPS-derived Caribbean-North America velocity in the vicinity of the strike-slip restraining bend of northern Hispaniola into components parallel and perpendicular to the plate boundary yields an even larger value, 12 ± 3 mm/yr for the boundary normal component [*DeMets et al.*, 2000].

[38] The resulting velocities of these two previous studies are and compared with the more densely spaced, observed GPS-derived velocities from this study in Figure 6c and Table 4. We find that *Lundgren and Russo*'s [1996] fault geometry and slip rates produce a very good fit with the GPS velocities for plate boundary-parallel motion, but a poor fit for plate boundary-normal motion. Moreover, the predictions of *Lundgren and Russo* [1996] exhibit a systematic rotation between predicted and measured velocities (Figure 6a).

[39] We find that *Dixon et al.*'s [1998] fault geometry and slip rates result in a good agreement with the GPS velocities for plate boundary-parallel motion (strike-slip component) (Figure 6b). Since no attempt was made to constrain fault-perpendicular motion, we make no comparison with our 3-D model.

[40] We conclude that both models resolve well the plate boundary-parallel motion in Hispaniola accommodated by the two inner, subaerial strike-slip faults (Septentrional, Enriquillo). The *Lundgren and Russo* [1996] model predicts significantly less plate-normal shortening than measured with GPS and probably accommodated by the outer, submarine thrust faults (North Hispaniola and Muertos) (Figure 2).

[41] The fact that *Lundgren and Russo* [1996] assume essentially strike-slip motion on all active faults across the plate boundary, including on the NHF and fail to reproduce the GPS-derived velocities, suggests that strike-slip motion through a simple restraining bend geometry is not sufficient to explain the present-day strain distribution in the northeastern Caribbean, particularly in Hispaniola. *Lundgren and Russo* [1996] include 2 to 6 mm/yr of thrust motion on the Muertos fault, decreasing from west to east, but this does not improve the fit to the observed GPS results.

[42] Possible interpretations of this misfit by *Lundgren and Russo* [1996] include (1) that elastic models are not sufficient to explain the velocities obtained by GPS, and that more complex models, including viscoelasticity and a realistic lithospheric structure and heat flow, are necessary; and (2) that a significant amount of shortening is accommodated either by thrust motion on the North Hispaniola-Puerto Rico fault or by diffuse shortening across the plate boundary.

3.5. Revised Best Fit Model

[43] In the following, we test whether an elastic strain model accounting for significant thrust motion on the North

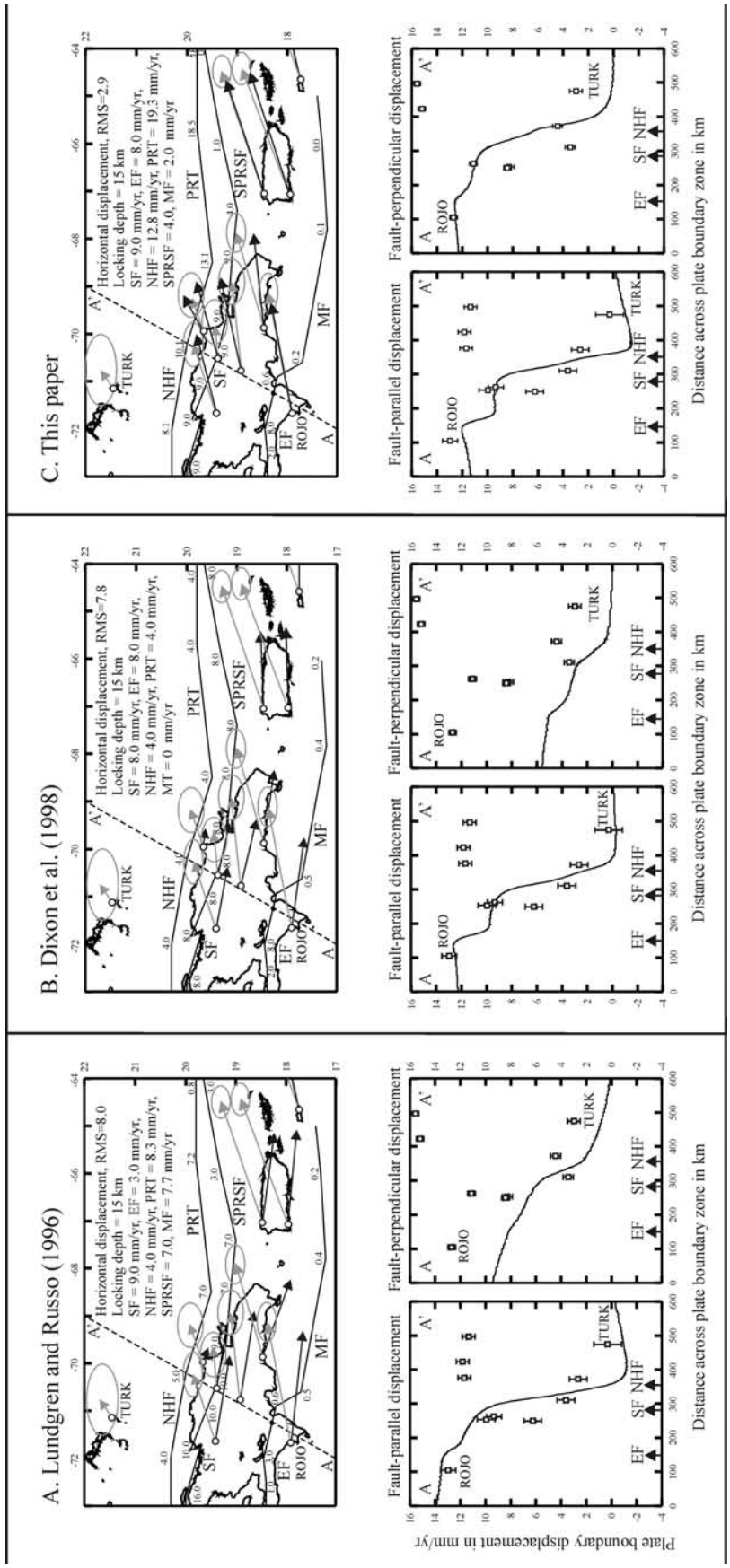

Figure 6. (a) Comparison of predicted GPS velocities from two-dimensional finite element model of *Lundgren and Russo* [1996] (black arrows) with observed GPS velocities (gray arrows with error ellipses) in the Hispaniola-Puerto Rico area. Major active strike-slip or thrust plate boundary faults are indicated: NHF, North Hispaniola fault; PRT, Puerto Rico trench; SPRSF, South Puerto Rico Slope fault; SF = Septentrional fault; EF = Enriquillo fault; MF = Muertos fault. Lower graphs show model-predicted fault-parallel and fault-perpendicular displacements (continuous, solid line) along profile A-A′ indicated by the dashed line in upper map. Small squares with error bars represent GPS site velocity data at locations shown in upper map. (b) Comparison of predicted GPS velocities from two-dimensional elastic model of *Dixon et al.* [1998] (black arrows) with observed GPS velocities (gray arrows with error ellipses). Lower graphs show model-predicted fault-parallel and fault-perpendicular displacements (continuous, solid line) along profile A-A′ indicated by the dashed line in upper map. Small squares with error bars represent GPS site velocity data at locations shown in upper map. (c) Comparison of predicted GPS velocities (black arrows) from our three-dimensional model in this paper with observed GPS velocities (gray arrows with error ellipses). Our model allows significant, margin-perpendicular thrusting along the North Hispaniola fault (Hispaniola-Bahama collision zone). Lower graphs show model-predicted fault-parallel and fault-perpendicular displacements (continuous, solid line) along profile A-A′ indicated by the dashed line in upper map. Small squares with error bars represent GPS site velocity data at locations shown in upper map. See text for discussion.

Table 4. Predicted Fault Slip Rates in Hispaniola and Surrounding Offshore Regions According to Models by *Lundgren and Russo* [1996] (cf. Figure 6a), *Dixon et al.* [1998] (cf. Figure 6b), and This Paper (cf. Figure 6c)[a]

		Fault Slip Rates, mm/yr					
	Locking Depth, km	Septentrional Fault	Enriquillo Fault	N. Hispaniola Fault	Puerto Rico Trench	Muertos Trough	RMS, mm/yr
Lundgren and Russo [1996], Figure 6a	15	10.0	3.0	4.0	8.3	7.7	8.0
Dixon et al. [1998], Figure 6b	15	8.0	8.0	4.0	not modeled	not modeled	7.8
This paper, Figure 6c	15	9.0	10.0	12.8	22.4	7.7	3.1

[a]Fault slip rates in mm/yr.

Hispaniola fault as mapped by *Dillon et al.* [1992] and *Dolan et al.* [1998] can fit the GPS-derived velocities in Hispaniola and Puerto Rico. We impose the fault geometry derived from geologic mapping summarized above along with the single slip rate on the Septentrional fault (9 mm/yr) [*Prentice et al.*, 2002] (Table 5). In addition, we use an additional external constraint by imposing that the total sum of the fault-parallel and fault-perpendicular velocities across the plate boundary zone in the model matches the prediction of the boundary-normal and boundary-parallel velocity component derived from the Caribbean-North American kinematic model of *DeMets et al.* [2000] (Figure 1b). We then estimate individual slip rates on other faults by trial and error. This approach, although it results in nonunique solutions, shows the following:

[44] A minimum slip rate of 9 mm/yr is necessary on the Enriquillo fault in order to account for the total left-lateral shear motion across the plate boundary, without violating GPS velocities in northern Hispaniola (Figure 6c and Table 4). Observed GPS velocities are violated if a strike-slip component larger than 9 mm/yr is placed on the Septentrional and/or the North Hispaniola-Puerto Rico trench fault).

[45] It is not possible to fit the plate boundary-normal shortening and direction of the GPS velocities without including a significant amount of reverse motion on the North Hispaniola fault.

[46] Our best fit model shown in Figure 6c predicts 12.8 mm/yr on the North Hispaniola fault, 9 mm/yr on the Septentrional fault, 10 mm/yr of left-lateral strike-slip motion on the Enriquillo fault, 7.7 mm/yr on the Muertos fault (decreasing in magnitude from west [Bahama collision area] to east [area outside of collision area]), and 22.4 mm/yr on the Puerto Rico trench fault. While the results of this modeling approach are of course highly nonunique, the modeling results demonstrate that it is possible to fit reasonably well the GPS-derived velocities in the northeastern Caribbean if a significant amount of collision-related thrusting is allowed on the North Hispaniola fault.

4. Discussion

4.1. Strain Partitioning in the Oblique Collision Zone Between Hispaniola and the Bahama Platform

[47] This analysis of the GPS results in terms of elastic strain accumulation has a direct bearing on strike-slip versus convergent deformation models in the northeastern Caribbean. We have shown that strike-slip models for Hispaniola neotectonics (i.e., convergent deformation is produced only by the restraining bend geometry of the plate boundary and motion on active faults are essentially purely strike-slip as proposed by *Mann et al.* [1984], *Calais and Mercier de Lépinay* [1993], *Russo and Villaseñor* [1995], and *Lundgren and Russo* [1996]) fail to reproduce the plate boundary normal shortening documented by the GPS velocities (Figure 6c). This misfit suggests that an additional tectonic process contributes to the current strain regime in the Hispaniola area. We find that the GPS velocities and a simple elastic strain model require a significant amount of thrust motion on the North Hispaniola fault (13 mm/yr or more), of the same magnitude, or greater, than strike-slip motion on the Septentrional fault or Enriquillo fault (Table 4). This result is consistent with a model of oblique collision between Hispaniola and the Bahamas platform, in which about half of the Caribbean-North America relative motion is accommodated by oblique

Table 5. Parameters Used for Faults Shown in Model in Figure 6c[a]

Fault Name	Lon1	Lat1	Lon2	Lat2	Dip	U1	U2
Septentrional fault	−72.8	20.0	−71.7	19.7	90	9	0
	−71.8	19.9	−71.0	19.6	90	9	0
	−71.0	19.6	−70.4	19.37	90	9	0
	−70.3	19.37	−69.6	19.2	90	9	0
	−69.6	19.2	−68.4	19.1	90	9	0
	−68.4	19.1	−67.4	19.0	90	9	0
	−67.4	19.0	−66.0	19.3	90	4	0
	−66.0	19.3	−64.0	19.65	90	1	0
North Hispaniola fault	−72.0	20.3	−70.2	20.0	30	8	10
	−70.2	20.0	−68.5	19.5	30	10	10
Puerto Rico trench	−68.5	19.5	−67.2	19.6	20	13	10
	−67.2	19.6	−65.7	19.8	20	13	10
	−65.7	19.8	−64.0	19.8	20	18	5
Enriquillo fault	−73.7	18.40	−72.5	18.40	90	8	0
	−72.5	18.40	−72.0	18.45	90	8	0
	−72.0	18.45	−70.9	18.2	90	8	0
Muertos fault	−70.9	18.2	−70.6	17.7	−20	0	6
	−70.6	17.7	−68.5	17.3	−20	0	2
	−68.5	17.3	−66	17.3	−20	0	1
	−66	17.3	−65	17.4	−20	0	0

[a]Definitions are as follows: Lon1, lat1, lon2, and lat2 are the coordinates of the end points of each of the fault segments. Dip is the fault dip in degrees (negative for north dipping faults). U1 is the strike-slip rate in mm/yr, U2 is the dip-slip rate in mm/yr. Locking depth was fixed to 15 km for all the faults.

slip on a relatively shallow dipping thrust fault at the interface between the two plates (Figure 6c).

[48] The fact that GPS-derived velocities favor a model with oblique slip on the North Hispaniola fault is also consistent with an abrupt variation in the type of earthquake slip vectors in the Hispaniola-Bahama convergent zone (Figure 2a). Large, instrumentally recorded earthquakes east of the convergent zone (whose eastern limit is taken as the Mona block at 68°W) show mostly low-angle thrust planes with slip vectors (Figure 2a) that are parallel to the east-northeast (070°) direction of Caribbean-North America plate motion derived by *DeMets et al.* [2000] (Figure 1b). These earthquakes appear to be representative of "normal" subduction of denser, thicker, older (Cretaceous) ocean floor beneath the Puerto Rico trench. West of 68°W in the Hispaniola-Bahamas collision zone, earthquakes show a more diverse mix of strike-slip and thrust fault planes indicative of strain partitioning on both thrust and strike-slip faults. *Dolan and Wald* [1998] argue that these larger magnitude and more complex events accompany the subduction of the Bahama Platform beneath northern Hispaniola.

[49] Oblique-slip motion on the North Hispaniola fault is also consistent with *Dolan and Wald*'s [1998] interpretation of the 4 August 1946, M_s = 8.1, earthquake offshore northeastern Hispaniola, the largest earthquake to affect the northern Caribbean plate boundary in the past 400 years (Figure 2a). *Dolan and Wald* [1998] interpret the event as an oblique left-lateral thrust on a gently south dipping plate interface fault (corresponding to the North Hispaniola fault) and with a slip vector trending 030–035°. *Russo and Villaseñor* [1995] argue for oblique-slip motion on a steeply northeastward dipping fault trending west-northwest, corresponding to the western prolongation of the Septentrional fault offshore Dominican Republic, with a slip vector trending due west, also consistent with the 9 mm/yr slip rate required by the elastic strain model and GPS velocities on the Septentrional fault (Table 4).

[50] In general, large historical earthquakes are confined to the area of Bahamas-Hispaniola convergence zone within and to the west of the Mona block as shown in Figure 4b. The occurrence of large earthquakes in the area of the convergence zone is consistent with the idea that subduction of bathymetric highs like the Bahamas Platform is generally accompanied by large thrust-type earthquakes related to increased frictional coupling between the highs and the base of the overriding plate [*Dolan et al.*, 1998].

4.2. Is the Slip Deficit in GPS Velocities From Hispaniola Evidence for a Detached Hispaniola Microplate or the Manifestation of Elastic Strain Effects Along Active Faults?

[51] GPS-derived velocities at five sites in central and eastern Hispaniola (CAPO, FRAN, CONS, MOCA, SDOM) show significant discrepancies with the prediction of a rigid Caribbean plate model as seen in the global, North American (Figure 3a), and Caribbean reference frames (Figure 3b). These sites have consistently more easterly strikes and slower rates than the sites in Puerto Rico, the Virgin Islands and the Lesser Antilles that are moving as part of the stable Caribbean plate [*Jansma et al.*, 2000]. Residual velocities in a Caribbean fixed frame (Figure 3b) illustrate this result with residual velocities of 5–14 mm/yr in a west–southwest direction.

[52] An important tectonic question becomes whether these anomalies are indicating the geologic impedance and detachment of a Hispaniola microplate against the Bahama Platform (i.e., permanent strain recorded in the geologic structure of the island) or whether these anomalies are simply a much shorter-term impedance of the Caribbean plate related to a slip deficit of major earthquakes (i.e., elastic strain recoverable during one or two major earthquakes). In the former microplate interpretation, the clockwise deflection of GPS velocities relative to sites in areas east of the convergent zone would indicate sideways motion of a detached Hispaniola block around the difficult to subduct, 22- to 27-km-thick crust of the Bahama Platform (Figure 4a).

[53] To attempt to answer this question, we describe young geologic structures in the areas bounding the zone of slow GPS velocities in central Hispaniola which record permanent strains and block motions over the past several million years. We argue that these structures which have developed to the east and south of Hispaniola over the past 3 to 5 million years support the possibility of microplate detachment in the collision zone. However, the GPS data taken alone remains ambiguous because of the complexities of elastic strains along active faults and therefore may not directly support the microplate hypothesis. Continued improvements in both the density of the Hispaniola and Puerto Rico GPS networks and the accuracy of velocities at these sites should help future studies to distinguish between permanent strains seen in young rock deformation and elastic strains imposed by the proximity of active faults. For the purpose of this paper, we use plate tectonic and geologic data to develop a tectonic model shown in Figures 9a–9d and point out areas of consistency and inconsistency between the geologic and GPS data.

4.3. Rifting Between Hispaniola and Puerto Rico in the Mona Passage

[54] Our best fit elastic strain model indicates strike-slip motion of 12.8 mm/yr and 9 mm/yr on the North Hispaniola fault and Septentrional fault, respectively (Figure 6c and Table 4). The model suggests that slip along the Septentrional fault decreases to the east and is taken up by very oblique subduction along the Puerto Rico trench. Similarly, the model suggests that left-lateral strike-slip motion along the Enriquillo fault decreases to zero as it connects to the east with the Muertos fault and accretionary prism (Figure 5a). This implies that the long-term eastward motion of the central part of Hispaniola (between the Septentrional and Enriquillo faults) relative to North America is slower than that of Puerto Rico. This difference in velocity must be accommodated by east–west extension within the Hispaniola-Puerto Rico area, either by diffuse deformation across the entire area, by localized deformation on active extensional structures, or a combination of the two processes.

[55] Figure 7a shows a bathymetric, tectonic, and earthquake epicenter map of the Puerto Rico-Virgin Islands area based on marine geophysical mapping by *Grindlay et al.* [1997] and *van Gestel et al.* [1998]. Faults in the Puerto Rico trench area trend east–northeast and reflect the path of the subducted southeast extension of the Bahama Platform along the northern edge the Caribbean forearc. These fault trends, which include both strike-slip faults, such as the North and South Puerto Rico Slope faults and low-angle thrusts like the Puerto Rico trench fault, parallel the present-day GPS velocity of Puerto Rico relative to North America (Figure 7a). The end of the now-subducted Bahama Platform (Mona block) coincides with the eastern edge of the Mona rift, a 25-km-wide full graben that has disrupted the Oligocene to early Pliocene carbonate platform. An incompletely mapped zone of northwest striking normal and oblique-slip faults extends to the south and southwest of the rift and deforms the carbonate platform in the central part of the Mona Passage. The carbonate platform is also deformed into the Puerto Rico-Virgin Islands arch whose structural crest parallels the topographically highest land areas of the Virgin Islands, Puerto Rico and eastern Hispaniola (Figure 7a).

[56] Our simplified interpretation of this complex pattern of deformation is shown schematically in Figure 7b. As the incoming Bahamas platform has obliquely subducted beneath the edge of the Caribbean plate, the subducting platform has indented a linear belt or buttress of underlying Eocene island arc rocks on the Caribbean plate in Hispaniola and the western Mona Passage. Complex rifting in the Mona Passage reflects rifting and rotation as the uncollided area to the east rotates in a counterclockwise direction. Paleomagnetic studies of the Neogene carbonate platform in Puerto Rico confirm 25° of counterclockwise (CCW) rotation of the island in late Miocene-Pliocene time [*Reid et al*, 1991]. The collided or ''impeded'' area of the Caribbean plate to the west of the Mona Passage undergoes widespread shortening while the uncollided area to the east of the Mona Passage in Puerto Rico and the Virgin Islands is characterized mainly by CCW rotation about a hinge point in the Mona Passage, broad arching of the Puerto Rico-Virgin Islands arch, normal faulting related to separation from the collided area, and strike-slip faulting. Available GPS data has not confirmed the occurrence of active CCW rotation in Puerto Rico [*Jansma et al.*, 2000].

[57] Seismic data across the Mona rift show that the largest normal displacement of the Oligocene-early Pliocene carbonate platform has occurred along the eastern boundary fault (Figure 7c). *van Gestel et al.* [1998] estimated 5.35 km of post-early Pliocene extension based on the seismic lines shown in Figure 9b and 6.35 km of extension on a line to the south that is not shown here. Assuming that the onset of extension in the Mona rift is post-early Pliocene (3.5 m.y.), this gives an average extension rate of about 2 mm/yr. However, if the normal faults are younger, than the opening rate is significantly faster. *Jansma et al.* [2000] used GPS results from western Puerto Rico and Hispaniola to estimate an opening rate of 5 mm/yr. For the amount of observed extension, this rate would indicate a minimum Pleistocene age (1.2 m.y.) for the initiation of rifting.

[58] In summary, these significant rates of predicted opening across the Mona Passage and the associated suite of rift structures shown in Figure 7a are consistent with the interpretation that the GPS velocities in central Hispaniola (Figure 4a) may reflect slowing or impedance of a detached Hispaniola microplate in response to the Bahama collision. The anomalous clockwise deviation of GPS velocities in Hispaniola seen in Figure 3a is also consistent with this interpretation.

4.4. Late Neogene Shortening of Hispaniola

[59] GPS velocities viewed in the framework of a fixed Caribbean plate in Hispaniola (FRAN, MOCA, CONS, CAPO, SDOM, ROJO) indicate that Hispaniola moves in a southwestwardly direction (220°) at a rate of 5–20 mm/yr (Figure 5a). The vector at ROJO on the southern coast of Hispaniola has a significantly slower rate than velocities to the north and is close in rate and direction to velocities to the west in Puerto Rico (ISAB, PARA), St. Croix, (CRO1), and the Lesser Antilles (GUAD, MART) (Figure 3b). This similarity over a large region suggests that these velocities are part of the stable Caribbean plate, a conclusion reached by *DeMets et al.* [2000] and *Jansma et al.* [2000]. Their small velocities could reflect a systematic error or could be a real expression of north–south convergence between the North America and Caribbean plates as proposed by *Dixon and Mao* [1997].

[60] The southwestward directions of GPS velocities in the Hispaniola area relative to the Caribbean plate is consistent with abundant evidence for late Neogene geologic shortening across the island and in offshore areas. These GPS velocities agree well with the geologically constrained direction of overthrusting which is known to be southwestward based on geologic and geophysical studies described below and summarized in Figures 8a–8e. Because the main component of thrusting is southwestward and subparallel to the convergence direction of the Bahama Platform into the collision zone, the main locus of deformation is in the area facing the colliding Bahama Platform south and southwest of Hispaniola and not in the area removed from the Bahama Platform in Puerto Rico, St. Croix and the Muertos trench as shown schematically in Figure 7b. This interpretation of the important kinematic role played by the colliding Bahama Platform is consistent with the interpretation by *Jansma et al.* [2000] that there is little or no differential movement in the areas removed from the collision (i.e., across the eastern Muertos trench and the Anegada fault between St. Croix and Puerto Rico).

[61] In the Hispaniola area, the lateral variation in GPS velocities along the length of the island may be related to differing basement thickness of oceanic plateau crust of the Caribbean Sea (Figure 5a). An abrupt change in crustal thickness from >20 km along the Beata Ridge to 5–10 km in the Haiti subbasin of *Mauffret and Leroy* [1997, 1999] may create a zone of right-lateral shear aligned along the landward extension of the Beata Ridge as seen by the slower SDOM vector relative to the much faster GPS

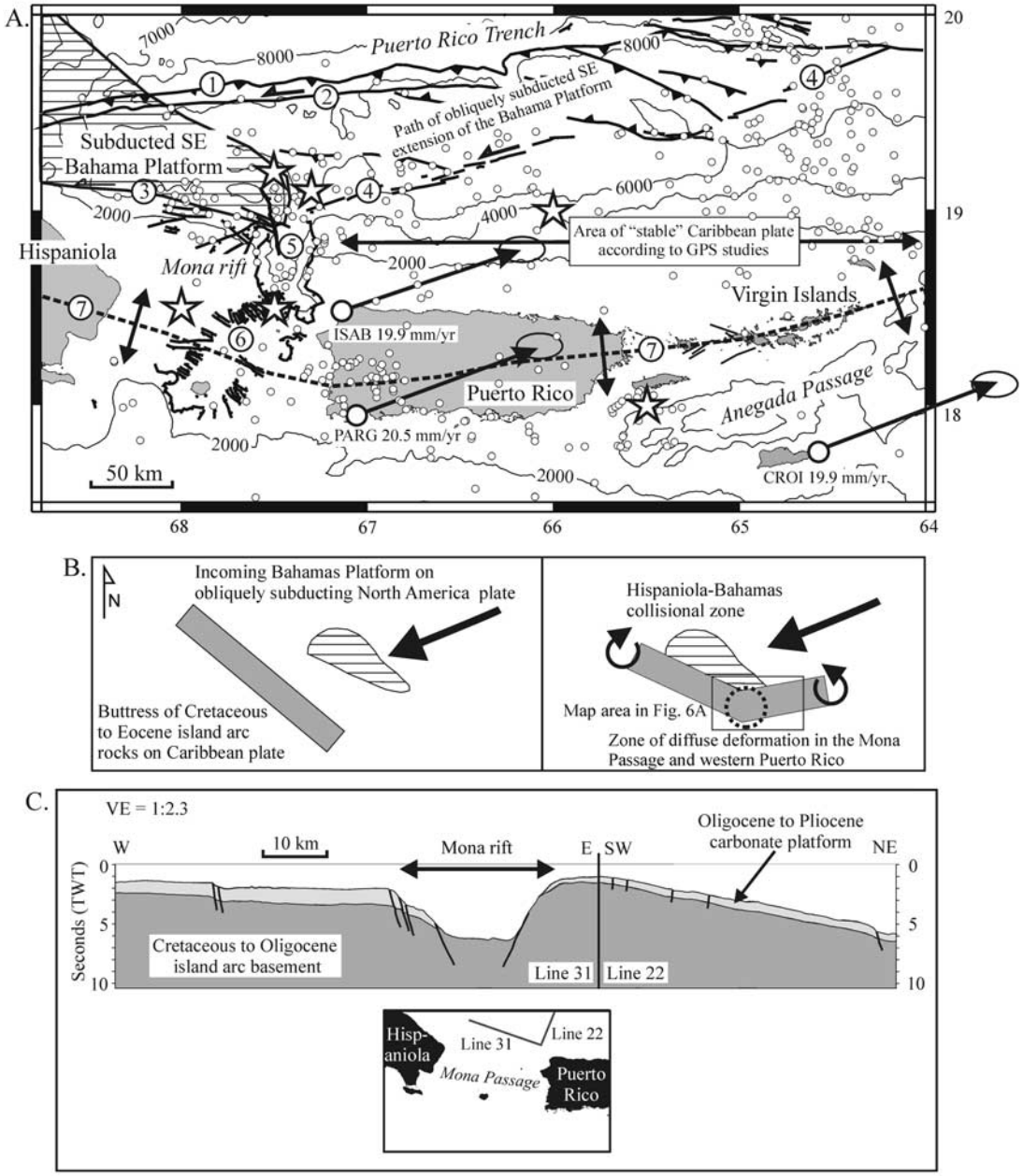

Figure 7. (a) Bathymetric and tectonic map of the eastern Hispaniola-Puerto Rico-Virgin Islands area modified from *Grindlay et al.* [1997] and *van Gestel et al.* [1998] showing faulting and earthquakes near the eastern edge of the Hispaniola-Bahama collision zone. Motions of GPS sites at St. Croix (CRO1), Parguera (PARG) and Isabella (ISAB) are indistinguishable from the larger Caribbean plate. Open circles are earthquake epicenters from 1973–1999 occurring at depths <30 km. Stars represent large-magnitude historic earthquakes. Key to numbered features: 1 = Puerto Rico trench; 2 = North Puerto Rico Slope fault; 3 = Septentrional fault; 4 = South Puerto Rico Slope fault; 5 = area of normal faults bounding the Mona rift; 6 = area of diffuse normal and oblique-slip faults in the Mona Passage; 7 = Puerto Rico-Virgin Islands arch. (b) Schematic diagram illustrating regional effect of oblique Bahama collision on the tectonics of the area of the Mona Passage and western Puerto Rico. Hispaniola has a post-middle Miocene history of crustal convergence related to the Bahama collision while the same period in Puerto Rico is dominated by extension probably related to a 25° CCW rotation that accompanied the collision and indentation of the buttress of ancient arc rocks in Hispaniola and Puerto Rico. (c) Approximately east-west single-channel seismic line across the Mona rift showing its localized disruption of an otherwise undeformed Oligocene-Pliocene carbonate cap.

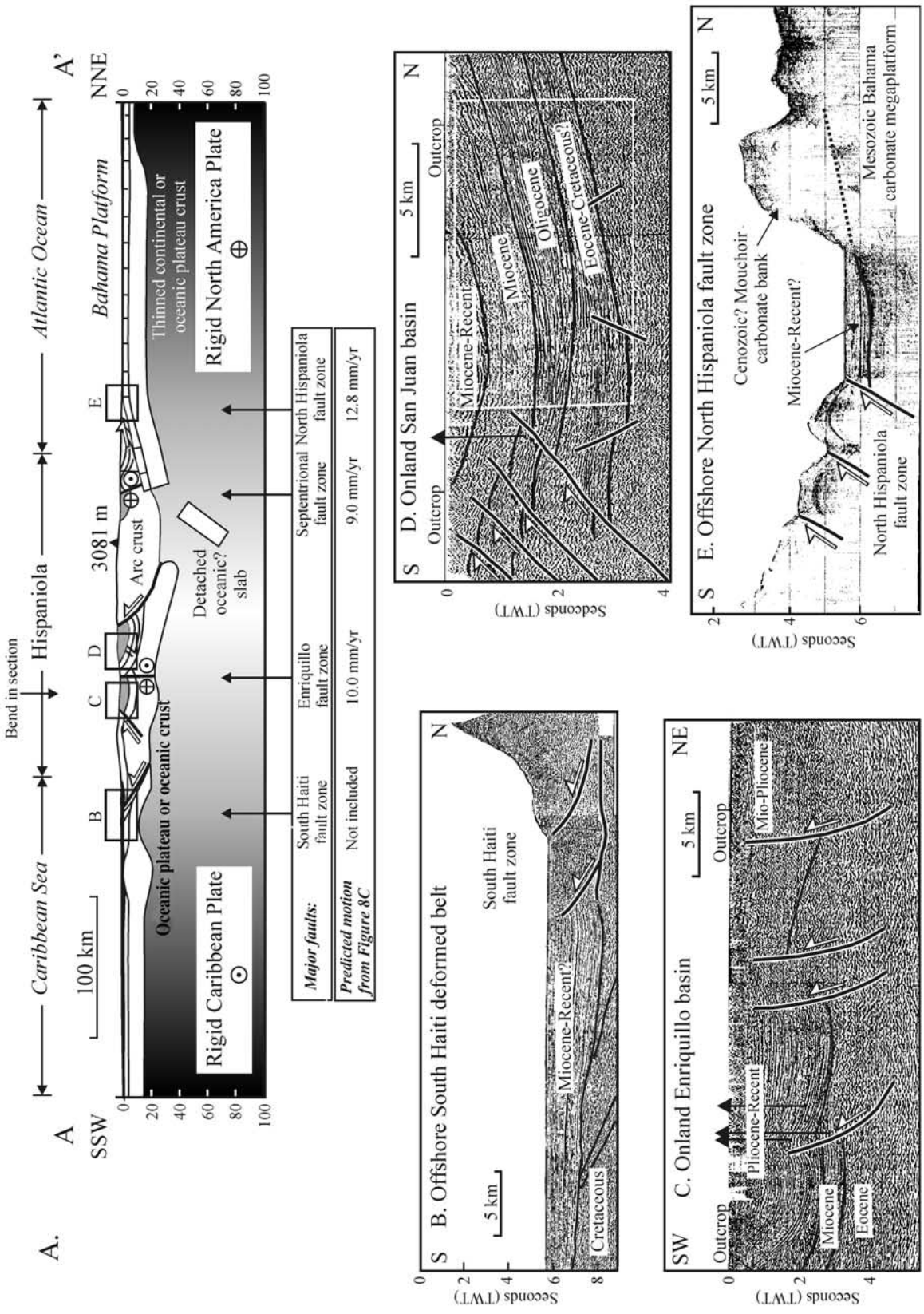
A.
A
SSW
Caribbean Sea
Bend in section
Hispaniola
Atlantic Ocean
A'
NNE
100 km
B
C
D
3081 m
E
Bahama Platform
Oceanic plateau or oceanic crust
Arc crust
Thinned continental or oceanic plateau crust
Detached oceanic? slab
Rigid Caribbean Plate
Rigid North America Plate
Major faults:
South Haiti fault zone
Enriquillo fault zone
Septentrional North Hispaniola fault zone
Predicted motion from Figure 8C
Not included
10.0 mm/yr
9.0 mm/yr
12.8 mm/yr
B. Offshore South Haiti deformed belt
South Haiti fault zone
Miocene-Recent?
Cretaceous
C. Onland Enriquillo basin
Outcrop
Pliocene-Recent
Mio-Pliocene
Miocene
Eocene
D. Onland San Juan basin
Miocene-Recent
Miocene
Oligocene
Eocene-Cretaceous?
E. Offshore North Hispaniola fault zone
Cenozoic? Mouchoir carbonate bank
Miocene-Recent?
Mesozoic Bahama carbonate megaplatform
North Hispaniola fault zone
5 km
Seconds (TWT)

velocities of central Hispaniola (Figure 3a). *Driscoll and Diebold* [1998] discuss the role of the Beata Ridge as a major active transform fault between areas of differing crustal thicknesses in the northern part of the Caribbean plate. The activity of the Beata Ridge in the central part of the Caribbean plate cannot be fully tested with present GPS data because there is only one GPS site in the stable area of the western Caribbean (SANA, Figure 1b).

[62] The southwestward thrusting of Hispaniola as a result of Bahama collision would be accommodated by (1) oblique convergence on the North Hispaniola fault; (2) strike-slip movement on the Enriquillo fault (estimated to be 10 mm/yr in the preferred elastic model; Figure 6c and Table 4); and (3) shortening of southern Hispaniola and western Muertos trench. We summarize a few of the salient geologic and structural characteristics of southern Hispaniola that are consistent with the model for Bahama Platform collision. The structure of the Enriquillo fault is summarized by *Mann et al.* [1995] and is not repeated here.

[63] Details and supporting references for key tectonic features in Hispaniola and its offshore areas are summarized in the cross section shown in Figure 8a and the accompanying seismic reflection sections which are aligned roughly along the line of section shown in Figure 5b. The cross section and accompanying seismic lines reveals several important features about the deformation in the area between faster GPS velocities in the area of central Hispaniola and the much slower vector at ROJO that is thought to move with the Caribbean plate (Figure 6a):

1. The most prominent folding and thrusting event in central Hispaniola is late Miocene and younger in age and verges southward to southwestward in a direction subparallel to the GPS velocities shown in Figure 5a. This direction of motion may reflect the presence of thinner crust in the Haiti subbasin (5–10 km) that is easier to overthrust than the thicker block of the Beata Ridge (>20 km) (Figure 3b). South to southwest vergence of the central mountain range of Hispaniola is reflected in its slightly asymmetric topographic profile with straighter and steeper slopes along its southwestern flank [*Mann et al.*, 1991] (Figure 8a). Thrusts in the Enriquillo basin dip northeastward and affect clastic sedimentary rocks as young as Pleistocene [*Mann et al.*, 1999] (Figure 8c). Older Oligocene and Miocene sedimentary units in the San Juan-Azua ramp basin show no thinning to the north or south and therefore support the idea that the onset of deformation occurred in Mio-Pliocene time [*Nemec*, 1980] (Figure 8d).

2. Late Miocene and younger reverse and oblique-slip faulting is responsible for the present pattern of morphotectonic units in central Hispaniola, including the distribution of the three major "ramp," or thrust-bound basins: the Enriquillo, San Juan-Azua, and the Cibao (Figure 8a). The steeper dipping flank of the San Juan-Azua basin is its northern flank (Figure 8d) in accordance with southwestward directed fault movement. The age of subsidence of the Enriquillo ramp basin has been studied by backstripping sedimentary well data from the 5-km-deep Charco Largo-1 well in the center of the basin [*Mann et al.*, 1999]. This study indicated that the main pulse of basement subsidence related to northeastward dipping thrusts seen on the seismic line in Figure 8c began about 5.5 m.y. ago and has continued to the present day. Sedimentation recorded in the well rapidly changes from deep marine late Miocene environments to shallow-marine to subaerial evaporitic environments formed in the closed intermontane setting of the ramp basin. Prior to this phase of late Miocene-Pliocene thrust related sedimentation, the area was characterized by pelagic carbonate deposition.

3. Unlike the apparently inactive Muertos fault south of eastern Puerto Rico and St. Croix, a zone of low-angle thrust faulting, the South Haiti fault appears to separate Hispaniola from the Caribbean plate (Figure 8b). The similarity between GPS velocities at ROJO in southernmost Hispaniola and stable sites in the Caribbean plate suggest that the amount of motion on the South Haiti deformed belt is smaller than the 2–3 mm/yr level of uncertainty in the velocity for ROJO.

[64] In summary, these geologic observations are consistent with the detachment of a Hispaniola microplate in the zone of maximum Caribbean North America plate conver-

Figure 8. (opposite) (a) Regional, schematic cross section extending from the Caribbean Sea across the North America-Caribbean plate boundary zone in Hispaniola to the Atlantic Ocean (line of section shown in Figure 5b; onland part of the section modified from *Mann et al.* [1991]). Seismic sections shown below in B, C, D, and E are located in Figure 8b–e. These lines were selected to show major crustal types and late Neogene structural features important to our interpretation of GPS results. (b) Multichannel seismic reflection line across the South Haiti fault zone at base of island slope from *Mauffret and Leroy* [1999]. Cretaceous oceanic plateau of the Haiti subbasin with crustal thickness of 8 km exhibits northward dipping reflectors formed by Cretaceous plateau lava flows. (c) Multichannel seismic reflection line across the 4.3-km-thick, late Miocene-recent Enriquillo basin from *Mann et al.* [1999]. Northeastward dipping thrust faults deform Miocene-Pleistocene clastic rocks, underlying Miocene-Eocene carbonate rocks, and likely oceanic plateau basement similar to the Haiti subbasin to the south. (d) Multichannel seismic reflection line across the San Juan basin modified from *Nemec* [1980]. Mio-Recent depocenter and synclinal basin structure is controlled by inward thrusting by adjacent mountain blocks as seen on the cross section in A. Steeper dipping limb to the northeast and Mio-Recent depocenter indicate Miocene and younger age of dominantly southwest directed thrust deformation. (e) Single-channel seismic reflection line across the North Hispaniola fault zone from *Dolan et al.* [1998]. Miocene-Recent? oblique subduction of the south tilted Mouchoir carbonate bank in the Bahamas is accompanied by formation of an accretionary wedge along the base of the island slope of northern Hispaniola.

gence (Figure 1b) by a combination of late Miocene to Recent thrusting, folding and strike-slip faulting along and adjacent to the Enriquillo and Muertos faults of southern Hispaniola. Motion along the Enriquillo-Muertos zone is assumed to be transferred to the extension in the Mona rift area in order to explain the lack of activity in the eastern Muertos trench south of Puerto Rico inferred by marine geophysical observations [*Masson and Scanlon*, 1991] and by GPS [*Jansma et al.*, 2000]. Motion of southwestern Hispaniola and Jamaica and its possible relation to central Hispaniola are being addressed by ongoing GPS studies by this group.

4.5. Rigidity of the Area of Puerto Rico, the Virgin Islands, and the Lesser Antilles

[65] Unlike Hispaniola, GPS velocities in the Puerto Rico, Virgin Islands and Lesser Antilles sites show that these areas are moving as part of the stable Caribbean plate, at least at the 2–3 mm/yr level (Figure 3). The conclusion that the Puerto Rico-Virgin Islands block moved as part of the stable Caribbean plate was also established by *Jansma et al.* [2000], who included 16 more campaign GPS sites from Puerto Rico and three continuously recording ones. *DeMets et al.* [2000] showed that Aves Island (AVES) in the eastern Caribbean moves with the stable Caribbean plate. Our results extend these conclusions to the entire Lesser Antilles volcanic arc and forearc area, at least in the area of Barbados Island (Figure 3).

[66] The behavior of the Puerto Rico-Virgin Islands and Lesser Antilles as a rigid block indicates very slow (<1.5 mm/yr) or no motion on the eastern part of the Muertos fault south of Puerto Rico and the Anegada Passage fault between Puerto Rico and St. Croix (Figure 2a). These results do not support tectonic models involving present-day rotation of the Puerto Rico-Virgin Islands block about a nearby vertical axis and/or eastward tectonic escape of a Puerto Rico-Virgin Islands microplate [*Jansma et al.*, 2000]. Indeed, rotation and tectonic escape models both predict (1) relative motion between the Puerto Rico-Virgin Islands and Lesser Antilles; (2) relative motion between the Puerto Rico-Virgin Islands and the Caribbean plate interior along the eastern Muertos fault; and (3) right-lateral strike slip motion along the northern boundary of the Puerto Rico-Virgin Islands block.

[67] Given that the present uncertainties in the GPS velocities we use, particularly in Puerto Rico, are approximately ±2–3 mm/yr, motion of the Puerto Rico-Virgin Islands block at rates slower than this could be occurring. Support for the idea of slow tectonic deformation of the area is given by recent evidence for late Holocene faulting in Puerto Rico [*Prentice et al.*, 2000] and in offshore areas including the shelf areas of western and southern Puerto Rico [*Grindlay et al.*, 2000], the deepwater Anegada Passage [*Jany et al.*, 1990] and areas of the Caribbean Sea south of Hispaniola [*Mauffret and Leroy*, 1999] (Figure 2a). Moreover, all of these areas have been affected by large historical earthquakes and tsunamis [*McCann and Sykes*, 1984]. Longer GPS time series eventually may permit us to address the question of whether slow motion of Puerto Rico relative to the Caribbean plate in the manner depicted schematically in Figure 7b is the mechanism for late Holocene faulting observed in Puerto Rico and its western and southern shelf areas [*Grindlay et al.*, 2000; *Prentice et al.*, 2000].

4.6. Integrated Model for the Recent Tectonic Evolution of the Northeastern Caribbean Plate

[68] In Figures 9a–9c, we reconstruct the Miocene to recent history of convergence between the northeastern Caribbean plate and Bahama Platform to illustrate a possible tectonic scenario to explain the present-day pattern of GPS velocities in the Hispaniola-Puerto Rico area (Figure 3). The four reconstructions present a simple two-plate model describing Caribbean-North America plate motion from the earliest Miocene (A) to the present-day (D). The Caribbean plate is held fixed while the North America plate is moved eastward by closing magnetic anomalies in the Cayman trough [*Leroy et al.*, 2000]. The fixed Caribbean frame is consistent with recent global plate models by *Müller et al.* [1999] suggesting that the Caribbean plate has remained fixed in a mantle reference frame for much of the Cenozoic while the North and South America plates have moved to the west past it. The Euler pole at 3.4 Ma is the GPS-derived pole of *DeMets et al.* [2000] which is also consistent with fault and magnetic anomaly data from the Cayman trough.

[69] We assume that the Mona block, which is highlighted on the reconstructions in the area of the northern Mona Passage, is the now subducted southeastern termination of the Bahama banks as discussed by previous workers including *McCann and Sykes* [1984] and *Dolan et al.* [1998]. In the Bahamas collisional model, areas to the west of the Mona block are potentially colliding with areas of Puerto Rico and Hispaniola, while areas to the east have recently collided. We have few constraints on the nature of crust in the large recess of the southern Bahamas that is now opposite northern Hispaniola. However, subducted slabs beneath eastern Hispaniola shown in Figure 2b

Figure 9. (opposite) Plate reconstructions of the Hispaniola-Bahamas collision zone for four intervals done using the UTIG PLATES software program. The Caribbean plate is held fixed and land area of Cuba (brown) and the Bahama carbonate platform (high-standing banks are dark blue, deeper bank areas are light blue) are moved with North America. An uncolored outline of the present-day land area of Cuba is shown on the North America plate for reference. Red dots are magnetic anomaly picks in oceanic crust of the Atlantic Ocean and Cayman trough. (a) Earliest Miocene (23.7 Ma); (b) Late Miocene (11.2 Ma); (c) Late Pliocene (3.4 Ma); and (d) Present. Key to numbered microplates in D: 1 = Hispaniola microplate; 2 = Septentrional microplate; 3 = Gonave microplate. Red dots and arrows in D show GPS site velocities relative to a fixed Caribbean plate. See text for discussion. See color version of this figure at back of this issue.

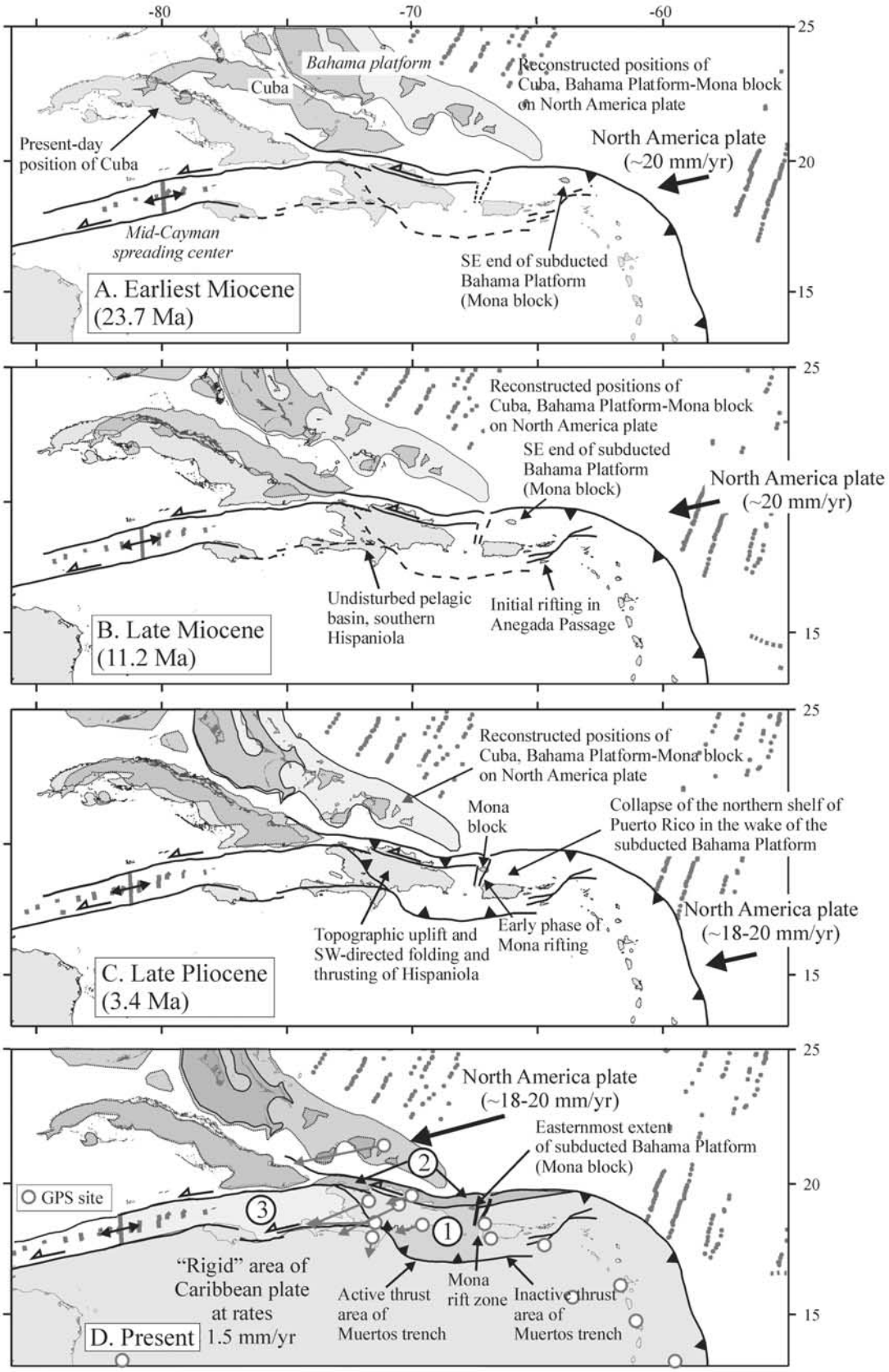
-80
-70
-60
25
20
15
Bahama platform
Cuba
Reconstructed positions of Cuba, Bahama Platform-Mona block on North America plate
Present-day position of Cuba
North America plate (~20 mm/yr)
Mid-Cayman spreading center
SE end of subducted Bahama Platform (Mona block)
A. Earliest Miocene (23.7 Ma)
Reconstructed positions of Cuba, Bahama Platform-Mona block on North America plate
SE end of subducted Bahama Platform (Mona block)
North America plate (~20 mm/yr)
Undisturbed pelagic basin, southern Hispaniola
Initial rifting in Anegada Passage
B. Late Miocene (11.2 Ma)
Reconstructed positions of Cuba, Bahama Platform-Mona block on North America plate
Mona block
Collapse of the northern shelf of Puerto Rico in the wake of the subducted Bahama Platform
North America plate (~18-20 mm/yr)
Topographic uplift and SW-directed folding and thrusting of Hispaniola
Early phase of Mona rifting
C. Late Pliocene (3.4 Ma)
North America plate (~18-20 mm/yr)
Easternmost extent of subducted Bahama Platform (Mona block)
GPS site
1
2
3
"Rigid" area of Caribbean plate at rates 1.5 mm/yr
Active thrust area of Muertos trench
Mona rift zone
Inactive thrust area of Muertos trench
D. Present

indicate at least 150–200 km of late Neogene plate convergence.

4.6.1. Early Collisional Effects in Puerto Rico Area and Eastern Muertos Trench

[70] In earliest Miocene to late Miocene time the Mona block area is moving from northeast to north of Puerto Rico in a roughly east–west direction (Figures 9a and 9b). The North Puerto Rico slope strike-slip fault, which parallels the present-day GPS North America-Caribbean plate direction (Figure 4a), appears to mark the surface trace of the Mona block as it passes beneath the forearc of northern Puerto Rico [*Grindlay et al.*, 1997]. There are few structural effects observed on the shelf of northern Puerto Rico during this interval although age constraints on offshore seismic sequences are imprecise [*van Gestel et al.*, 1998]. *Gill et al.* [1999] note that the earliest rifting observed in St. Croix adjacent to the Anegada Passage east of Puerto Rico began in the late Middle Miocene. Tectonic erosion related to the oblique subduction of the Mona block is a possible mechanism for the widespread collapse of the northern Puerto Rico carbonate shelf about 3.5 Ma. In the middle to early part of the late Miocene, much of southern Hispaniola is covered by a pelagic carbonate basin recording tectonic quiescence.

4.6.2. Later Collisional Effects in Hispaniola and Western Muertos Trench

[71] By the late Pliocene, the Mona block is northeast of Puerto Rico and the carbonate shelf has collapsed in its wake. During this time, rifting may have begun in the Mona Passage (Figure 9c) and Hispaniola experienced major topographic uplift and southwestward directed folding and thrusting as summarized in Figures 8a–8e. In northern Hispaniola, a late Miocene-early Pliocene carbonate bank similar in age and lithology to the one in the Puerto Rico and Mona Passage area was uplifted and folded following its deposition as a tabular unit [*Calais and Mercier de Lépinay*, 1991; *De Zoeten and Mann*, 1991]. In the present, GPS data indicates active extension between Puerto Rico and Hispaniola at rates as fast as 5 mm/yr that are consistent with late Neogene rift structures [*Jansma et al.*, 2000]. In a Caribbean frame, GPS velocities in Hispaniola show southwestward directions and fast velocities consistent with the pattern of folding, thrusting, and strike-slip faulting in southern Hispaniola (Figure 5a).

[72] Crustal convergence across Hispaniola appears to have been accompanied by the detachment of the slabs at depth beneath central and eastern Hispaniola and the Mona Passage (Figures 2a and 2b). Slab breakoff may have been a response to the inability of thicker crust of the Bahama Platform to be subducted beneath Hispaniola as shown schematically in Figure 8a.

4.6.3. Present-Day Area of Rigid Caribbean Plate

[73] The east to west passage of the southeastern end of the Bahama Platform may explain the present-day rigid area of Puerto Rico and the Virgin Islands and lack of active subduction along the eastern Muertos trench [*Masson and Scanlon*, 1991; *Jansma et al.*, 2000], because Bahama-related deformational effects have largely subsided as the oblique collisional contact zone between the southeastern Bahamas and the Caribbean plate has migrated westward with time. The present-day juxtaposition of rifting in the Mona Passage at the inferred edge of the collision zone is consistent with the hypothesis that the collision has impeded the forward progress of the northeastern Caribbean plate and formed a microplate. The existence and exact boundaries of this microplate is a topic for future GPS studies in western Hispaniola (Haiti) and (Jamaica) (Figure 2a).

4.7. Comparison of Northeastern Caribbean to Tectonically Similar Areas

[74] The overall shape of the Lesser Antilles volcanic arc in the eastern Caribbean (Figure 1a) is similar to other volcanic arcs like the Marianas and Scotia (Figures 10b and 10c). These and other arcs are shaped like the letter "D" with a bulging curvature on the trenchward side and straight margin on the side adjacent to the site of the older remnant arc (Figures 10b and 10c). *Vogt et al.* [1976], *Hsui and Youngquist* [1985], and *McCann and Habermann* [1989] have pointed out that this distinctive shape could result from the arc becoming "pinned" by ridges of thickened crust at its ends. This situation results in the arc bulging through the unimpeded gap by a combination of subduction at the front of the arc and back arc spreading behind it as shown schematically in Figure 10a.

[75] The tectonic "pinning" process occurs because the extra buoyancy provided to the downgoing plate by its ridge of thickened crust gives the subducting plate a greater resistance to sinking than the adjacent, thinner oceanic crust. "Pinning points" are commonly "large igneous provinces," or anomalously thick areas of ocean crust, as compiled by *Vogt et al.* [1976], *McCann and Habermann* [1989], and *Coffin and Eldholm* [1994]. Examples of large igneous provinces acting as pinning points include the Ogasawara Plateau and Caroline Ridge in the Marianas area (Figure 10b) and the Northeast Georgia Rise in the Scotia area (Figure 10c). It is unknown whether the Bahama carbonate platform adjacent to Hispaniola is underlain by thinned continental crust, a large igneous province, or both.

[76] The shapes of pinned arcs seen on gravity maps in Figure 10 suggest that the arcs are in various stages of tectonic evolution and invite comparison to the Hispaniola area of the northeastern Caribbean. The Marianas arc appears to be in the juvenile stages of oblique collision for several reasons: (1) the reentrant in the plate boundary is small (particularly in the case of the northern Marianas); (2) there are no elevated landmasses adjacent to the pinned areas; (3) there is little evidence for convergent and strike-slip faulting; and (4) there is no evidence for a broken or detached slab in the mantle [*Stern and Smoot*, 1998]. The northeastern Scotia plate and the northeastern Caribbean appear to be in a more advanced state of oblique collision than the Marianas area as indicated by the presence of major reentrants in the trend of the plate boundaries and the presence of anomalously elevated land areas adjacent to the pinning points (Northeast Georgia Rise and Bahama

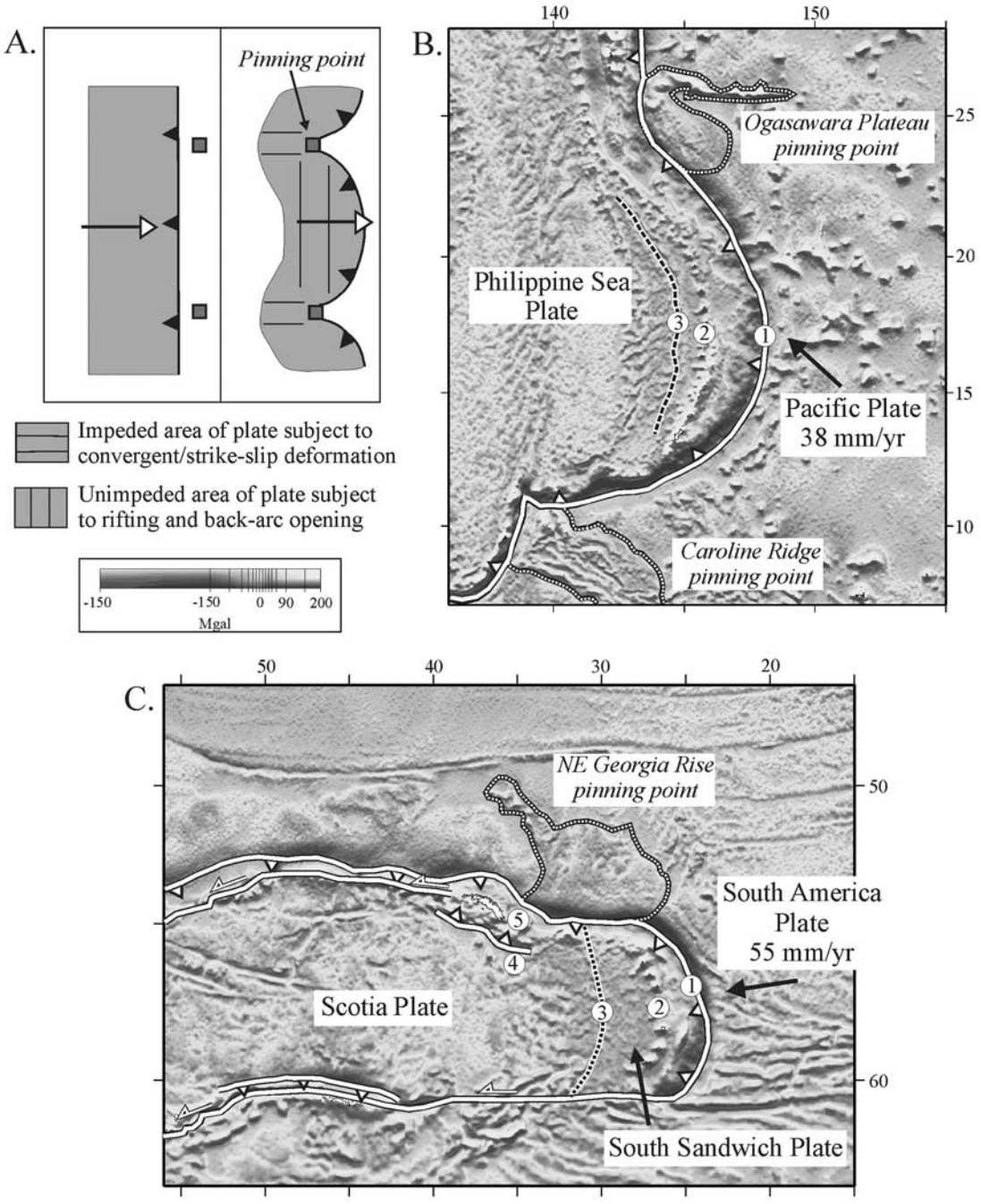

Figure 10. (a) Conceptual model for deformation of an arc by pinning at thicker than normal ridges on oceanic crust (red squares) (modified from *Marshak* [1988]). (b) Pinning of the Marianas arc at its northern and southern ends by the Ogasawara Plateau and the Caroline Ridge. Base map is a satellite-derived gravity map of the Caribbean compiled by *Sandwell and Smith* [1997]. Key to numbered features: 1 = Marianas trench; 2 = Marianas volcanic arc; 3 = Marianas back arc basin. (c) Pinning of the Scotia plate by oblique subduction of the Northeast Georgia Rise, a large igneous province on the seafloor of the South Atlantic Ocean. Key to numbered features: 1 = South Sandwich trench; 2 = South Sandwich arc; 3 = East Scotia back arc basin; 4 = possible backthrust southwest of South Georgia Island; 5 = South Georgia Island. See text for discussion. See color version of this figure at back of this issue.

Platform, respectively). Hispaniola has a maximum elevation of 3081 m on a 100–250-km-wide, 76,000 km^2 landmass and is known to be elevated by active thrusting in the Bahama-Hispaniola collision zone (Figure 8). South Georgia Island has a maximum elevation of 2934 m on a 3500 km^2, 50-km-wide landmass and is assumed to be undergoing regional convergence related to the indentation of the Scotia plate of the Northeast Georgia Rise. As in the case of eastern Hispaniola, a prominent bathymetric trench and a thrust earthquake southwest of South Georgia Island may be forming as the result of backthrusting of the South Georgia area southwestward over the Scotia plate [*Pelayo and Wiens*, 1989] (Figure 10c).

[77] Unlike the northeastern Caribbean, the Marianas area does not exhibit any obvious rift boundaries separating the impeded area of the plate adjacent to the pinning point and the unimpeded area of the plate (Figure 10a). *Vogt et al.* [1976] proposes that the East Scotia Sea back arc basin, presently opening at spreading rates now known to be 65–75 mm/yr [*Barker*, 1995], began about 15 million years ago as a result of initial oblique collision between the Northeast Georgia Rise and the Scotia plate. If this is the case, there is a similarity between this proposed oblique collision-induced mode of back arc rifting between the Scotia and South Sandwich plates and late Neogene rifting observed in the Mona Passage between the collided plate area in Hispaniola and the uncollided part of the plate in Puerto Rico. However, it appears unlikely the Mona rifting will eventually propagate and transversely split the entire plate in the manner proposed by *Vogt et al.* [1976] for the Scotia and South Sandwich plates because the Mona rifting is affecting a crustal block isolated above south and north dipping slabs of the North America and Caribbean plates, respectively (Figures 2a and 2b). The Grenada back arc basin is present to the west of the Lesser Antilles arc but this basin formed in Paleogene time and is presently inactive. More geologic, geophysical, and GPS-based geodetic studies are needed in the northeastern Caribbean and in analogous areas like the Scotia and Marianas regions to clarify the active and ancient tectonic processes and evolutionary stages of arcs following their encounters with pinning points of various sizes, compositions, and crustal thicknesses.

5. Conclusions

[78] The major conclusions of this paper are as follows:

1. GPS velocities in the northeastern Caribbean show two areas of significantly different mechanical behavior (Figures 3, 4, and 5). The Puerto Rico-Virgin Islands-Aves Island area is currently behaving as rigid block moving with the Caribbean plate at the 2–3 mm/yr level. Its rigid behavior indicates that these areas are far enough removed from the subduction front and its locked zone to minimize elastic strain associated with the subduction process. Rigid plate behavior including lack of elastic strain in the forearc is consistent with the presence of a little deformed Oligocene-early Pliocene carbonate platform over much of the area of eastern Puerto Rico and the Virgin Islands. The Hispaniola area is moving with the Caribbean plate but at significantly slower velocities. The boundary between the slower-moving Hispaniola area and the faster-moving Puerto-Virgin Islands area relative to the North America plate is the Mona Passage, where normal and oblique-slip faults deform the Oligocene-early Pliocene carbonate platform.

2. The GPS-derived velocity field in Hispaniola is compatible with a model of elastic strain accumulation along four major, roughly east–west striking fault zones which are locked to a depth of 15 km (Figure 6c). From north to south, these faults include the offshore North Hispaniola fault, the onland Septentrional fault, the onland Enriquillo fault, and the offshore Muertos fault. GPS-derived velocities favor a strain-partitioning model with oblique slip on the North Hispaniola and Muertos faults and strike-slip on the Septentrional and Enriquillo faults assuming elastic deformation on locked faults only. Low-angle oblique slip on the offshore faults is supported by offshore seismic reflection studies and earthquake slip vectors of large 20th century earthquakes. The high-angle strike-slip character of the Septentrional and Enriquillo faults is supported by field mapping along both structures.

3. GPS-derived velocities also require significant (>10 mm/yr) convergence (>10 mm/yr) on the North Hispaniola fault. This observation is consistent with marine geophysical studies showing a zone of collisional deformation separating the Bahamas Platform from the Hispaniola island slope. An oblique collisional model for Hispaniola neotectonics appears more consistent with both GPS and geologic data sets than either a simple strike-slip bend model [*Mann et al.*, 1984] or a model involving north–south convergence between the North and South American plates [*Dixon and Mao*, 1997].

4. Plate reconstructions combined with geologic observations show that the Bahama-Hispaniola oblique collision could result in the detachment of a fragment of the Caribbean plate opposite the thickest area of the Bahama Platform in Hispaniola (Figures 9a–9d). Pliocene and younger zones of normal faulting east of Hispaniola and zones of strike-slip, thrusts, and folds south of Hispaniola are consistent with relatively slower GPS velocities and the idea that Hispaniola is impeded against the Bahamas collision zone. However, at the present time we lack GPS constraints to effectively isolate elastic strain effects on faults that could contribute to the observed slip deficit area of GPS velocities in central Hispaniola. Moreover, we lack critical GPS data from the western edge of the microplate in Haiti and Jamaica to fully test the microplate hypothesis.

5. Potential seismic hazards are distributed over a wide geographic area because of the length of fault boundaries in the Mona Passage, northern Hispaniola and southern Hispaniola. Potential earthquake sources would include all of the microplate boundaries including the Enriquillo fault zone, the Mona rift and the North Hispaniola fault. The Enriquillo fault was spatially associated with a time-transgressive, east-to-west series of large historical ruptures between 1751 and 1860. The Mona rift is the presumed site

of the 1918 earthquake affecting western Puerto Rico and the North Hispaniola fault is [was?] the site of the 1943–1953 earthquake series which are the largest recorded earthquakes in the northern Caribbean. GPS results indicate that seismic hazard is much greater on Hispaniola where rates of shortening are much higher than in the adjacent uncollided area of Puerto Rico and the Virgin Islands. Seismic risks are especially large because of the dense and urbanized populations of Hispaniola, Puerto Rico and the Virgin Islands which have a combined population of about 21 million people.

6. Comparisons with tectonically similar areas indicate that the northeastern Caribbean is in an intermediate state of development adjacent to the "pinning point" of the Bahama Platform. A juvenile state of oblique collision is exemplified by the northern and southern ends of the Marianas arc where there are no large landmasses and no evidence for regional convergence or plate fragmentation. A similar state of development to the northeastern Caribbean is the northeastern Scotia arc where there is an elevated landmass, evidence for backthrusting, and a possible active rift boundary separating the collided and uncollided parts of the plate (East Scotia back arc basin).

[79] **Acknowledgments.** Funding for GPS-based tectonic studies in the Greater Antilles, Bahamas, and Aves Island was provided by individual NSF grants to R. Bilham (University of Colorado-Boulder), C. DeMets, P. Jansma, G. Mattioli, and P. Mann. P. Jansma and G. Mattioli were also supported at the University of Puerto Rico by NSF-EPSCOR, NSF-CREST, NSF-MRCE, and NASA (grant NCCW-0088). Initial funding for the GPS network was provided by NASA to T. Dixon. Funding to E. Calais was provided by a grant from INSU-CNRS "Tectoscope-Positionnement" program. We thank T. Dixon, B. Mercier de Lépinay, and C. Larroque for their assistance in all aspects of this study including data acquisition, data processing, and discussions of tectonic interpretations. We thank A. Lopez, L. Peña, the Dirección General de Minería, and the Instituto Cartográfico Militar for their continued support of GPS data acquisition in the Dominican Republic. Mann thanks the French Academy of Sciences and the Elf-Aquitaine Company for a visiting fellowship at CNRS-Géosciences Azur. We would like to thank U. ten Brink and R. Bennett for constructive reviews and C. Jones and B. Wernicke for their editorial efforts. UTIG contribution 1591.

References

Barker, P. F., Tectonic framework of the East Scotia Sea, in *Backarc Basins*: *Tectonics and Magmatism*, edited by B. Taylor, pp. 281–314, Plenum, New York, 1995.

Boucher, C., Z. Altamimi, and P. Sillard, The 1997 International Terrestrial Reference Frame (ITRF97), *IERS Tech. Note 27*, Paris Observatory, Paris, France, 1999.

Byrne, D. B., G. Suarez, and W. R. McCann, Muertos trough subduction–Microplate tectonics in the northern Caribbean?, *Nature*, *317*, 420–421, 1985.

Calais, E., and B. Mercier de Lépinay, From transpression to transtension along the northern Caribbean plate boundary: Implications for the recent motion of the Caribbean plate, *Tectonophysics*, *186*, 329–350, 1991.

Calais, E., and B. Mercier de Lépinay, Semiquantitative modeling of strain and kinematics along the Caribbean-North America strike-slip plate boundary zone, *J. Geophys. Res*, *98*, 8293–8308, 1993.

Calais, E., N. Bethoux, and B. Mercier de Lépinay, From transcurrent faulting to frontal subduction: A seismotectonic study of the northern Caribbean plate boundary from Cuba to Puerto Rico, *Tectonics*, *11*, 114–123, 1992.

Calais, E., J. Perrot, and B. Mercier de Lépinay, Strike-slip tectonics and seismicity along the northern Caribbean plate boundary from Cuba to Hispaniola, in *Active Strike-Slip and Collisional Tectonics of the Northern Caribbean Plate Boundary Zone*, edited by J. F. Dolan and P. Mann, *Spec. Pap. Geol. Soc. Am.*, 326, 125–141, 1998.

Coffin, M. F., and O. Eldholm, Large igneous provinces: Crustal structure, dimensions, and external consequences, *Rev. Geophys.*, *32*, 1–36, 1994.

DeMets, C., and T. H. Dixon, New kinematic models for Pacific-North America motion from 3 Ma to present, 1, Evidence for steady motion and biases in the NUVEL-1A model, *Geophys. Res. Lett.*, *26*, 1921–1924, 1999.

DeMets, C., R. G. Gordon, D. F. Argus, and S. Stein, Effect of recent revisions of the geomagnetic reversal timescale on estimates of current plate motions, *Geophys. Res. Lett.*, *21*, 2191–2194, 1994.

DeMets, C., P. Jansma, G. Mattioli, T. Dixon, F. Farina, R. Bilham, E. Calais, and P. Mann, GPS geodetic constraints on Caribbean-North America plate motion, *Geophys. Res. Lett.*, *27*, 437–440, 2000.

Deng, J., and L. R. Sykes, Determination of Euler pole for contemporary relative motion of Caribbean and North American plates using slip vectors of interplate earthquakes, *Tectonics*, *14*, 39–53, 1995.

De Zoeten, R., and P. Mann, Structural geology and Cenozoic tectonic history of the central Cordillera Septentrional, Dominican Republic, in *Geologic and Tectonic Development of the North America-Caribbean Plate Boundary in Hispaniola*, edited by P. Mann, G. Draper, and J. F. Lewis, Spec. Pap. Geol. Soc. Am., 262, 265–279, 1991.

Dillon, W. P., J. A. Austin Jr., K. M. Scanlon, and D. F. Coleman, Structure and development of the insular margin north of western Hispaniola: A tectonic accretionary wedge on the Caribbean plate boundary, *Mar. Pet. Geol.*, *9*, 70–88, 1992.

Dillon, W. P., N. T. Edgar, K. M. Scanlon, and L. M. Parson, A review of the tectonic problems of the strike-slip northern boundary of the Caribbean plate and examination by GLORIA, in *Geology of the United States Seafloor*: *The View from Gloria*, edited by J. V. Gardner, M. E. Field, and D. C. Twichell, pp. 135–164, Cambridge Univ. Press, New York, 1994.

Dixon, T. H., and A. Mao, A GPS estimate of relative motion between North and South America, *Geophys. Res. Lett.*, *24*, 535–538, 1997.

Dixon, T. H., G. Gonzalez, S. M. Lichten, and E. Katsigris, First epoch geodetic measurements with the Global Positioning System across the northern Caribbean plate boundary zone, *J. Geophys. Res.*, *96*, 2397–2415, 1991.

Dixon, T. H., F. Farina, C. DeMets, P. Jansma, P. Mann, and E. Calais, Relative motion between the Caribbean and North American plates and related plate boundary deformation based on a decade of GPS observations, *J. Geophys. Res.*, *103*, 15,157–15,182, 1998.

Dolan, J. F., and D. J. Wald, The 1943–1953 north-central Caribbean earthquakes: Active tectonic setting, seismic hazards and implications for Caribbean-North America plate motions, in *Active Strike-Slip and Collisional Tectonics of the Northern Caribbean Plate Boundary Zone*, edited by J. F. Dolan and P. Mann, Spec. Pap., Geol. Soc. Am., 326, 143–169, 1998.

Dolan, J. F., H. T. Mullins, and D. J. Wald, Active tectonics of the north-central Caribbean: Oblique collision, strain partitioning, and opposing subducted slabs, in *Active Strike-Slip and Collisional Tectonics of the Northern Caribbean Plate Boundary Zone*, edited by J. F. Dolan and P. Mann, Spec. Pap. Geol. Soc. Am., 326, 1–61, 1998.

Driscoll, N. W., and J. B. Diebold, Deformation of the Caribbean region: One plate or two?, *Geology*, *26*, 1043–1046, 1998.

Edgar, N. T., Structure and geologic development of the Cibao Valley, northern Hispaniola, in *Geologic and Tectonic Development of the North America-Caribbean Plate Boundary in Hispaniola*, edited by P. Mann, G. Draper, and J. F. Lewis, Spec. Pap. Geol. Soc. Am., 262, 281–299, 1991.

Feigl, K., and E. Dupré, RNGGHN: A program to calculate displacement components from dislocations in an elastic halfspace with applications for modeling geodetic measurements of crustal deformation, *Comput. Geosci.*, *25*, 695–704, 1999.

Gill, I., P. P. McLaughlin Jr., and D. K. Hubbard, Evolution of the Kingshill basin of St. Croix, U.S. Virgin Islands, in *Sedimentary Basins of the World*, vol. 4, *Caribbean Basins*, edited by P. Mann, pp. 343–366, Elsevier Sci., New York, 1999.

Grindlay, N. R., P. Mann, and J. F. Dolan, Researchers investigate submarine faults north of Puerto Rico, *Eos Trans. AGU*, *78*, 404, 1997.

Grindlay, N. R., L. Abrams, P. Mann, and L. Del Greco, A high-resolution sidescan and seismic survey reveals evidence of late Holocene fault activity offshore western and southern Puerto Rico, *Eos Trans. American Geophysical Union*, *81*(48), Fall Meet. Suppl., Abstract T11B-05, 2000.

Hsui, A. T., and S. Youngquist, A dynamic model of the curvature of the Mariana trench, *Nature*, *318*, 455–457, 1985.

Jansma, P. E., A. Lopez, G. S. Mattioli, C. DeMets, T. H. Dixon, P. Mann, and E. Calais, Neotectonics of Puerto Rico and the Virgin Islands, northeastern Caribbean, from GPS geodesy, *Tectonics*, *9*, 1021–1037, 2000.

Jany, I., K. M. Scanlon, and A. Mauffret, Geological interpretation of combined Seabeam, GLORIA, and seismic data from Anegada Passage (Virgin Islands, North Caribbean), *Mar. Geophys. Res.*, *12*, 173–196, 1990.

Jordan, T. H., The present-day motions of the Caribbean plate, *J. Geophys. Res.*, *80*, 4433–4449, 1975.

Leroy, S., A. Mauffret, P. Patriat, and B. Mercier de Lépinay, An alternative interpretation of the Cayman trough evolution from a reidentification of magnetic anomalies, *Geophys. J. Int.*, *141*, 539–557, 2000.

Lundgren, P. R., and R. M. Russo, Finite element modeling of crustal deformation in the North America–Caribbean plate boundary zone, *J. Geophys. Res.*, *101*, 11,317–11,327, 1996.

Mann, P., K. Burke, and T. Matumoto, Neotectonics of Hispaniola: Plate motion, sedimentation, and seismicity at a restraining bend, *Earth Planet. Sci. Lett.*, *70*, 311–324, 1984.

Mann, P., G. Draper, and J. F. Lewis, An overview of the geologic and tectonic development of Hispaniola, in *Geologic and Tectonic Development of the North America–Caribbean Plate Boundary in Hispaniola*, edited by P. Mann, G. Draper, and J. F. Lewis, Spec. Pap. Geol. Soc. Am., 262, 1–28, 1991.

Mann, P., F. W. Taylor, R. L. Edwards, and T. L. Ku, Actively evolving microplate formation by oblique collision and sideways motion along strike-slip faults: An example from the northwestern Caribbean plate margin, *Tectonophysics*, *246*, 1–69, 1995.

Mann, P., C. S. Prentice, G. Burr, L. R. Peña, and F. W. Taylor, Tectonic geomorphology and paleoseismology of the Septentrional fault system, Dominican Republic, in *Active Strike-Slip and Collisional Tectonics of the Northern Caribbean Plate Boundary Zone*, edited by J. F. Dolan and P. Mann, Spec. Pap. Geol. Soc. Am., 326, 63–123, 1998.

Mann, P., P. P. McLaughlin Jr., W. van den Bold, S. R. Lawrence, and M. E. Lamar, Tectonic and eustatic controls on Neogene evaporitic and siliciclastic deposition in the Enriquillo basin, Dominican Republic, in *Sedimentary Basins of the World*, vol. 4, *Caribbean Basins*, edited by P. Mann, pp. 287–342, Elsevier Sci., New York, 1999.

Mao, A., C. G. A. Harrison, and T. H. Dixon, Noise in GPS coordinate time series, *J. Geophys. Res.*, *104*, 2797–2816, 1999.

Marshak, S., Kinematics of orocline and arc formation in thin-skinned orogens, *Tectonics*, *7*, 73–86, 1988.

Masson, D. G., and K. M. Scanlon, The neotectonic setting of Puerto Rico, *Geol. Soc. Am. Bull.*, *103*, 144–154, 1991.

Mauffret, A., and S. Leroy, Seismic stratigraphy and structure of the Caribbean igneous province, *Tectonophysics*, *283*, 61–104, 1997.

Mauffret, A., and S. Leroy, Neogene intraplate deformation of the Caribbean plate at the Beata Ridge, in *Sedimentary Basins of the World*, vol. 4, *Caribbean Basins*, edited by P. Mann, pp. 627–669, Elsevier Sci., New York, 1999.

McCaffrey, R., Oblique plate convergence, slip vectors, and forearc deformation, *J. Geophys. Res.*, *97*, 8905–8915, 1992.

McCann, W. R., and R. E. Habermann, Morphologic and geologic effects of the subduction of bathymetric highs, *Pure Appl. Geophys.*, *129*, 41–69, 1989.

McCann, W. R., and L. R. Sykes, Subduction of aseismic ridges beneath the Caribbean plate: Implications for the tectonics and seismic potential of the northeastern Caribbean, *J. Geophys. Res.*, *89*, 4493–4519, 1984.

Molnar, P., and L. R. Sykes, Tectonics of the Caribbean and Middle America regions from focal mechanisms and seismicity, *Geol. Soc. Am. Bull.*, *80*, 1639–1684, 1969.

Müller, R. D., J. Y. Royer, S. C. Cande, W. R. Roest, and S. Maschenkov, New constraints on the Late Cretaceous/Tertiary plate tectonic evolution of the Caribbean, in *Sedimentary Basins of the World*, vol. 4, *Caribbean Basins*, edited by P. Mann, pp. 33–59, Elsevier Sci., New York, 1999.

Nemec, M. C., A two phase model for the tectonic evolution of the Caribbean, *Trans. Caribb. Geol. Conf.*, *9th*, 23–34, 1980.

Pelayo, A. M., and D. A. Wiens, Seismotectonics and relative plate motions in the Scotia Sea area, *J. Geophys. Res.*, *94*, 7293–7320, 1989.

Pollitz, F. F., and T. H. Dixon, GPS measurements across the northern Caribbean plate boundary: Impact of postseismic relaxation following historic earthquakes, *Geophys. Res. Lett.*, *25*, 2233–2236, 1998.

Prentice, C. S., P. Mann, F. W. Taylor, G. Burr, and S. Valastro, Paleoseismology of the North America-Caribbean plate boundary (Septentrional fault), Dominican Republic, *Geology*, *21*, 49–52, 1993.

Prentice, C. S., P. Mann, and G. Burr, Prehistoric earthquakes associated with a Late Quaternary fault in the Lajas Valley, southwestern Puerto Rico, *Eos Trans. American Geophysical Union*, *81*(48), Fall Meet. Suppl., Abstract T11B-10, 2000.

Prentice, C. S., P. Mann, L. Peña, and G. Burr, Slip rate and earthquake recurrence along the central Septentrional fault, North American-Caribbean plate boundary, Dominican Republic, *J. Geophys. Res.*, *107*, doi:10.1029/2001JB000442, in press, 2002.

Reid, J. A., P. W. Plumley, and J. H. Schellekens, Paleomagnetic evidence for late Miocene counterclockwise rotation of North Coast carbonate sequence, Puerto Rico, *Geophys. Res. Lett.*, *18*, 565–568, 1991.

Rosencrantz, E., and P. Mann, SeaMARC II mapping of transform faults in the Cayman trough, Caribbean Sea, *Geology*, *19*, 690–693, 1991.

Russo, R. M., and A. Villaseñor, The 1946 Hispaniola earthquake and the tectonics of the North America-Caribbean plate boundary zone, northeastern Hispaniola, *J. Geophys. Res.*, *100*, 6265–6280, 1995.

Sandwell, D. T., and W. H. F. Smith, Marine gravity anomaly from Geosat and ERS-1 satellite altimetry, *J. Geophys. Res.*, *102*, 10,039–10,054, 1997.

Savage, J. C., Strain accumulation in western United States, *Annu. Rev. Earth Planet Sci.*, *368*(11), 11–43, 1983.

Savage, J. C., Equivalent strike-slip earthquake cycles in halfspace and lithosphere asthenosphere Earth models, *J. Geophys. Res.*, *95*, 4873–4879, 1990.

Stern, R. J., and N. C. Smoot, A bathymetric overview of the Mariana forearc, *Island Arc*, *7*, 525–540, 1998.

Sykes, L. R., W. R. McCann, and A. L. Kafka, Motion of Caribbean plate during last 7 million years and implications of earlier Cenozoic movements, *J. Geophys. Res.*, *87*, 10,656–10,676, 1982.

van Gestel, J. P., P. Mann, J. F. Dolan, and N. R. Grindlay, Structure and tectonics of the upper Cenozoic Puerto Rico-Virgin Islands carbonate platform as determined from seismic reflection studies, *J. Geophys. Res.*, *103*, 30,505–30,530, 1998.

Vogt, P. R., A. Lowrie, D. R. Bracey, and R. N. Hey, Subduction of aseismic oceanic ridges: Effects on shape, seismicity, and other characteristics of consuming plate boundaries, *Spec. Pap. Geol. Soc. Am.*, *172*, 1–59, 1976.

E. Calais, Department of Earth and Atmospheric Sciences, Purdue University, Civil-1397, West Lafayette, IN 47907, USA. (ecalais@purdue.edu)

C. DeMets, Department of Geology and Geophysics, University of Wisconsin, Madison, WI 53706, USA. (chuck@geology.wisc.edu)

P. E. Jansma, Department of Geosciences, University of Arkansas, Fayetteville, AR 72701, USA. (pjansma@uark.edu)

P. Mann, Institute for Geophysics, University of Texas at Austin, 4412 Spicewood Springs Road, Bldg. 600, Austin, TX 78759-8500, USA. (paulm@ig.utexas.edu)

G. S. Mattioli, Department of Geology, P. O. Box 9017, University of Puerto Rico, Mayaguez, PR 00681-9017, USA. (glen@antigua.uprm.EDU)

J.-C. Ruegg, Laboratoire de Tectonique, CNRS-UMR 7578, Institut de Physique de Globe de Paris, 4 Place Jussieu, F-75252 Paris cedex, France. (ruegg@ipgp.jussieu.fr)

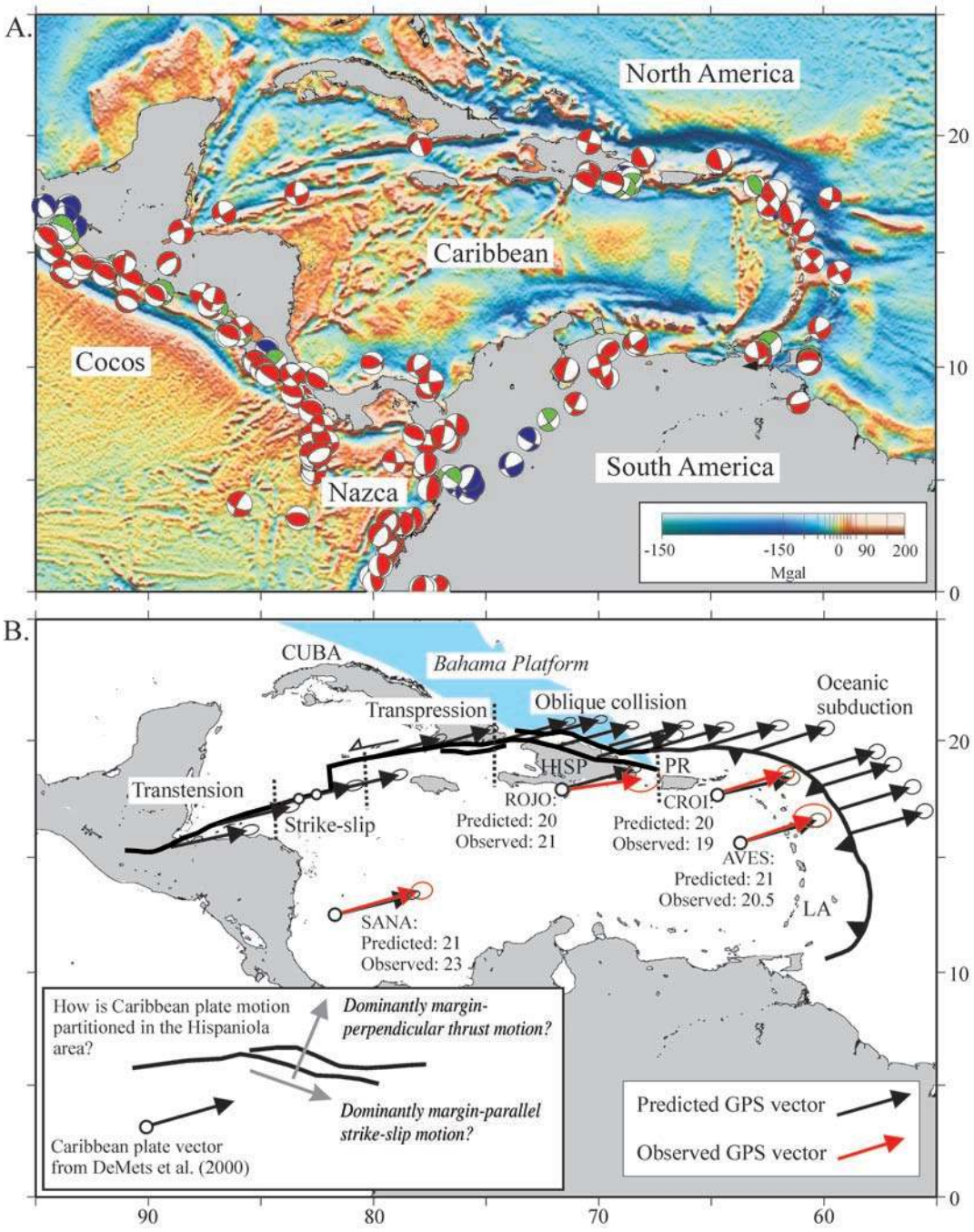

Figure 1. (a) Major plates of the Caribbean region and compilation of earthquake focal mechanisms showing present-day plate kinematics. Base map is a satellite-derived gravity map of the Caribbean compiled by *Sandwell and Smith* [1997]. Focal mechanisms shown in red are from earthquakes from 0 to 75 km in depth; blue mechanisms are from earthquakes 75 to 150 km in depth; and green mechanisms are >150 km in depth. (b) Caribbean-North America velocity predictions of *DeMets et al.* [2000] (black arrows) based on GPS velocities at four sites in the stable interior of the plate (red vectors) and two fault strike measurements in the strike-slip segment of the North America-Caribbean boundary (open circles). The predicted velocities are consistent with the along-strike transition in structural styles from transtension in the northwestern corner of the plate to oblique collision between the Caribbean plate in the Hispaniola (HISP) and Puerto Rico (PR) region and the Bahama Platform. One of the main objectives of this paper is to use GPS-based geodesy to determine how this motion is partitioned into margin-parallel strike-slip and margin-perpendicular thrust motions as shown in the inset diagram.

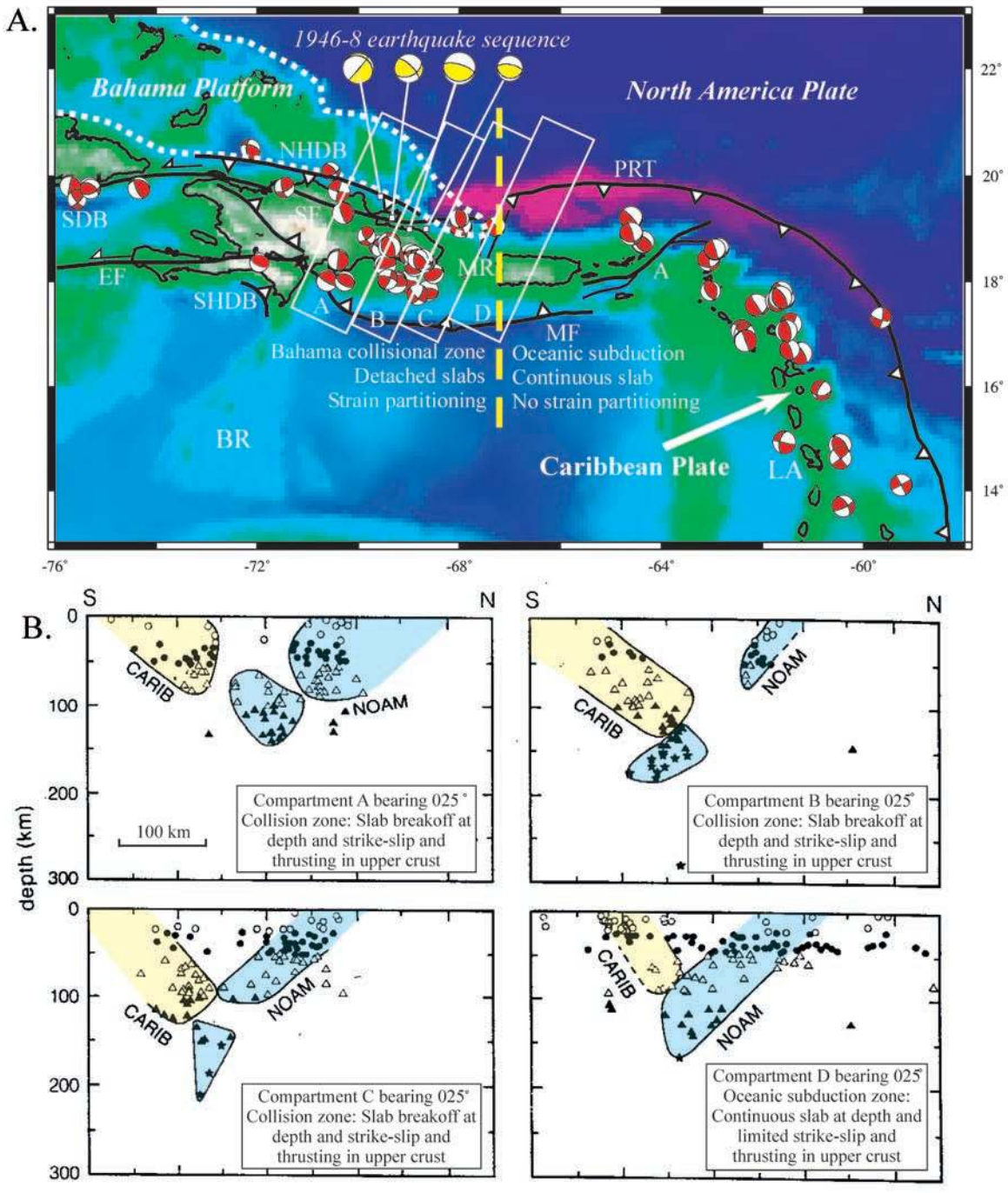

Figure 2. (a) Earthquake focal mechanisms along the northeastern margin of the Caribbean plate compared to the Caribbean-North America convergence direction. Focal mechanisms are from earthquakes from 0 to 50 km in depth: mechanisms in yellow are 1946-8 earthquake sequence [*Dolan and Wald*, 1998]; red mechanisms are compiled from the CMT catalogue [*Calais et al.*, 1992; *Molnar and Sykes*, 1969]. Most earthquake focal planes indicate thrusting along low-angle fault planes perpendicular to the *DeMets et al.* [2000] plate vector in the region of oceanic subduction east of the yellow, dashed line parallel to 67°W. West of this line, focal planes indicate strike-slip and oblique thrusting along variably oriented fault planes suggestive of strain partitioning within the Hispaniola-Bahama collision zone. (b) Plots of earthquake hypocenters in the Bahama Platform-Hispaniola-Puerto Rico collisional zone projected to planes passing through each of the compartments shown on the map in A (modified from *Dillon et al.* [1994]). Inferred tectonic setting, slab geometry, and crustal deformational style of each compartment is summarized in inset.

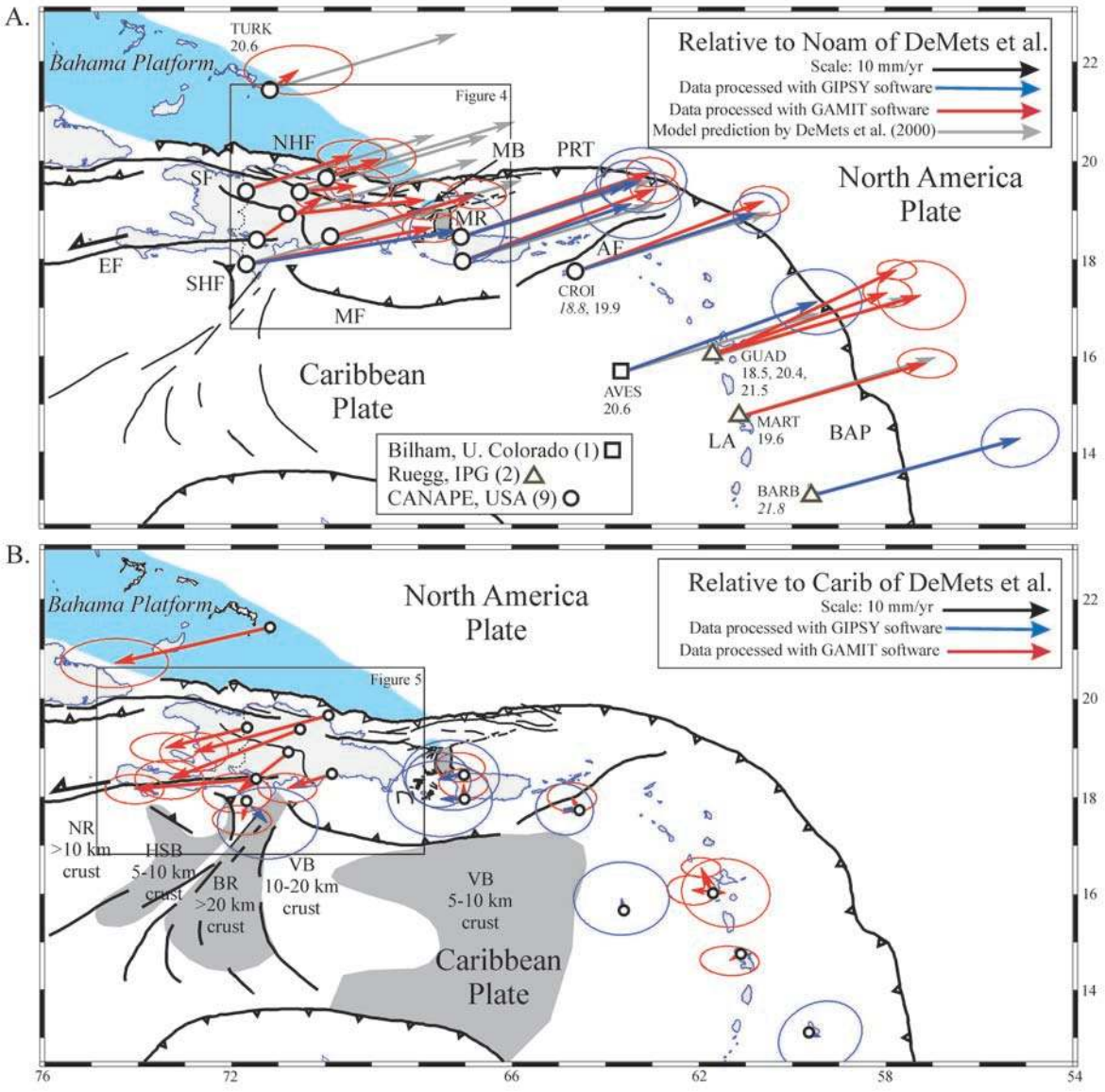

Figure 3. (a) Comparison of observed GPS velocities for Caribbean sites relative to North America. Color code for velocities shown in inset. Abbreviations for GPS sites: BARB, Barbados; MART, Martinique; GUAD, Guadeloupe; AVES, Aves Island; CRO1, St. Croix, U.S. Virgin Islands; TURK, Turk Island, Bahamas. Abbreviations of tectonic features: BAP, Barbados accretionary prism; LA, Lesser Antilles volcanic arc; AF, Anegada fault; PRT, Puerto Rico trench; MR, Mona rift (gray area); MF, Muertos fault; MB, Mona block; NHF, North Hispaniola fault; EF, Enriquillo fault; SHF, South Haiti fault. (b) Comparison of observed GPS velocities relative to the stable Caribbean plate as defined by *DeMets et al.* [2000]. Velocities show a strong southwestward component consistent with southwestward thrusting of late Miocene to recent age in Hispaniola. Variations in the crustal thickness of the Caribbean oceanic plateau on the Caribbean plate as determined by *Mauffret and Leroy* [1997] are shown. Abbreviations: NR, Nicaraguan Rise; HSB, Haiti subbasin; BR, Beata Ridge; VB, Venezuelan basin.

Figure 4. (opposite) (a) Crustal tectonic features of the Hispaniola-Bahama collision zone in Hispaniola (HISP, includes Dominican Republic and Haiti) compared with GPS velocities relative to the North America. Abbreviations for GPS sites: PARG, Parguera, Puerto Rico; ISAB, La Isabela, P.R.; SDOM, Santo Domingo, Dominican Republic; ROJO, Cabo Rojo, D.R.; COLO, Colorado, D.R.; CONS, Constanza, D.R.; CAPO, Capotillo, D.R.; MOCA, Moca, D.R.; FRAN, Cabo Frances Viejo, D.R. The velocities straddle the boundary of the Hispaniola-Bahama collisional zone, whose eastern limit is defined by the subducted carbonate high of the Bahama Platform, the Mona Block (MB), and the adjacent Mona rift (MR). The now-subducted Mona block is collinear with presumably similar carbonate highs to the northwest: the Navidad (NB), Silver (SB), and Mouchoir (MB) Banks. These banks grew to sea level on top of a broad, Mesozoic carbonate ''megaplatform'' now at an average depth of 4000 m. Active tectonic features of the overriding plate include thrust faults of the North Hispaniola fault (NHF) and Puerto Rico trench (PRT), the North Puerto Rico Slope (NPRSF), the South Puerto Rico Slope (SPRSF), the Septentrional (SF) and the Enriquillo (EF) left-lateral strike-slip faults, the Puerto Rico-Virgin Islands (PRVI) arch, the Mona rift, and the Muertos fault (MF). (b) Subcrustal tectonic features of the Hispaniola-Bahamas collision zone include three areas of the subducted North America slab reproduced from *Dillon et al.* [1994]: an area of a continuous subducted slab in the east; an area of detached slab in the center; and an area to the west where no slab has been mapped. The 1943–1953 earthquakes (stars) and their magnitudes are in the general area of the continuous subducted slab and probably represent increased coupling between the carbonate banks on the downgoing plate and the overriding Caribbean plate in Hispaniola.

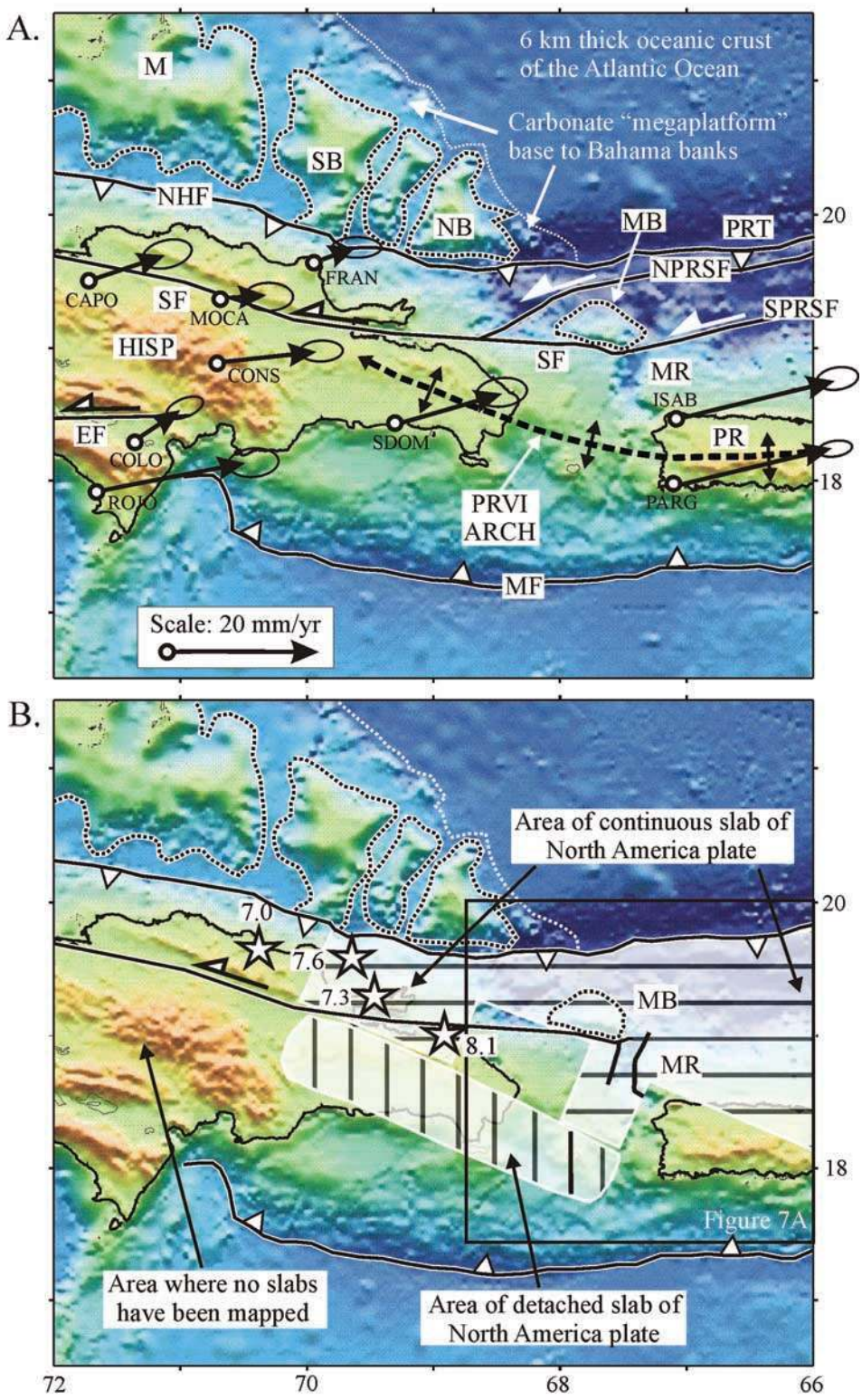
A.
6 km thick oceanic crust of the Atlantic Ocean
Carbonate "megaplatform" base to Bahama banks
M
SB
NHF
NB
MB
PRT
NPRSF
SPRSF
FRAN
CAPO
SF
MOCA
HISP
CONS
SF
MR
ISAB
EF
COLO
SDOM
PR
ROJO
PRVI ARCH
PARG
MF
Scale: 20 mm/yr
20
18
B.
Area of continuous slab of North America plate
7.0
7.6
7.3
8.1
MB
MR
Figure 7A
Area where no slabs have been mapped
Area of detached slab of North America plate
20
18
72
70
68
66

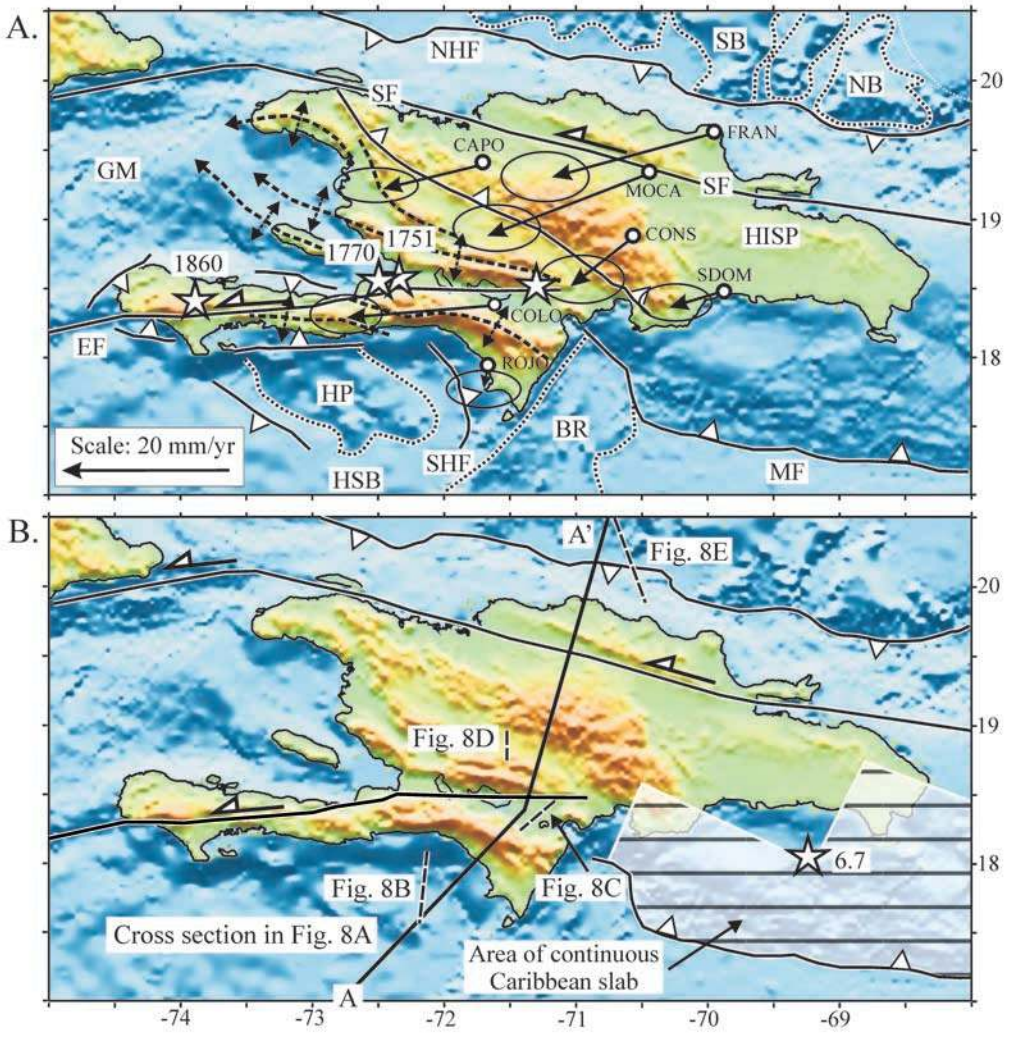

Figure 5. (a) Crustal tectonic features of the Hispaniola-Bahama collision zone compared with GPS velocities relative to the Caribbean plate reference frame. The velocities provide good across-strike coverage of the fold-thrust belt structure of Hispaniola (HISP) which represents southwestward backthrusting produced by the oblique collision of Hispaniola with the Bahama Platform. Stars represent a time-space progression of large historical earthquakes spatially associated with the Enriquillo fault that began in 1751 and extended westward to 1860. Abbreviations: SB, Silver Bank; NB, Navidad Bank; NHF, North Hispaniola fault; SF, Septentrional fault; EF, Enriquillo fault; SHF, South Haiti fault; BR, Beata Ridge; MT, Muertos fault; HP, Haiti Plateau; HSB, Haiti subbasin; GM, Gonave microplate. B. Subcrustal tectonic features of the Hispaniola-Bahama collision zone include an area of subducted Caribbean slab reproduced from *Dillon et al.* [1994]. The 1984 M6.7 thrust event occurred at a depth of 32 km and confirmed northward thrusting of the Caribbean plate beneath southeastern Hispaniola.

Figure 9. (opposite) Plate reconstructions of the Hispaniola-Bahamas collision zone for four intervals done using the UTIG PLATES software program. The Caribbean plate is held fixed and land area of Cuba (brown) and the Bahama carbonate platform (high-standing banks are dark blue, deeper bank areas are light blue) are moved with North America. An uncolored outline of the present-day land area of Cuba is shown on the North America plate for reference. Red dots are magnetic anomaly picks in oceanic crust of the Atlantic Ocean and Cayman trough. (a) Earliest Miocene (23.7 Ma); (b) Late Miocene (11.2 Ma); (c) Late Pliocene (3.4 Ma); and (d) Present. Key to numbered microplates in D: 1 = Hispaniola microplate; 2 = Septentrional microplate; 3 = Gonave microplate. Red dots and arrows in D show GPS site velocities relative to a fixed Caribbean plate. See text for discussion.

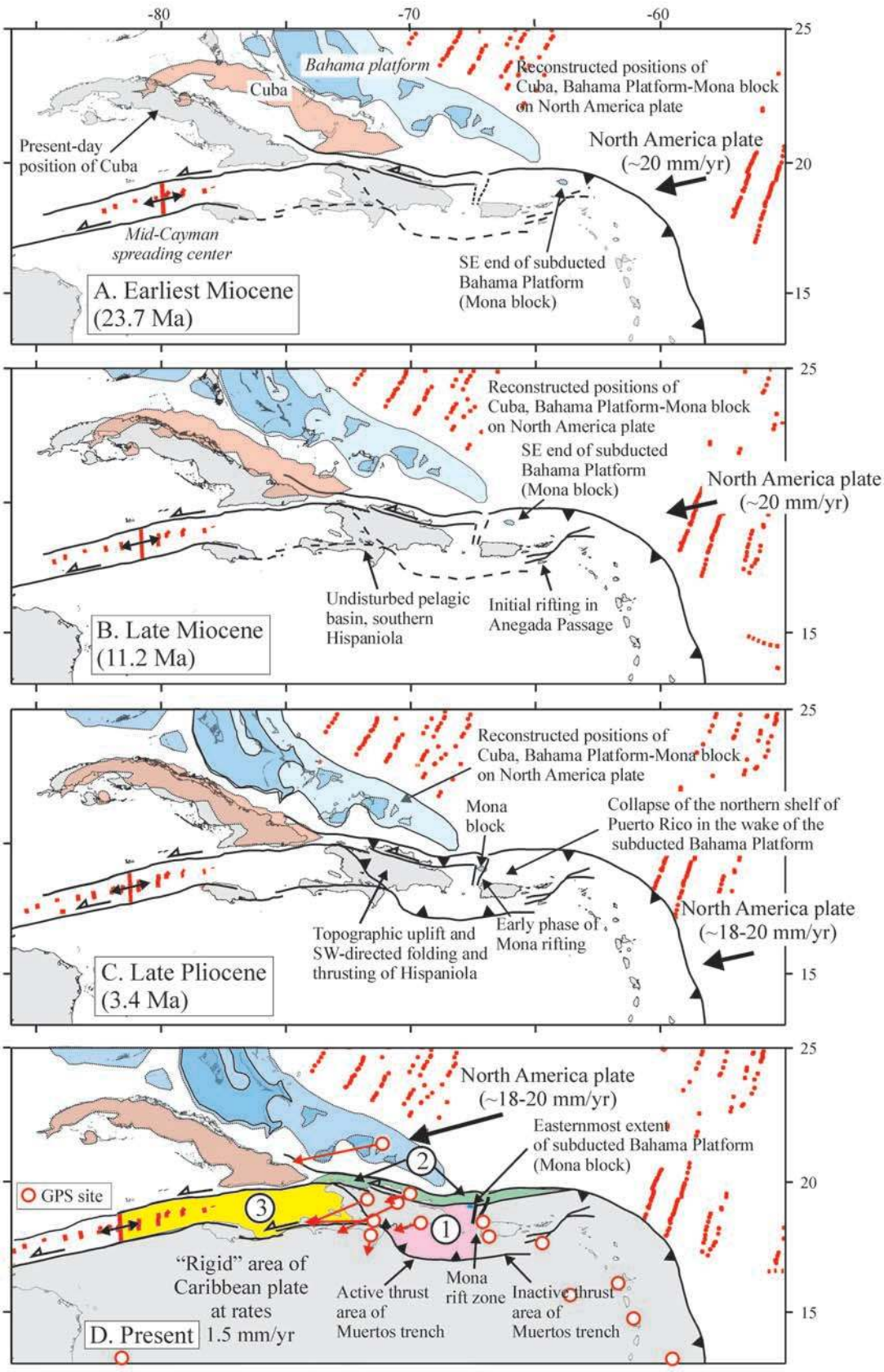
-80
-70
-60
25
20
15
Bahama platform
Cuba
Reconstructed positions of Cuba, Bahama Platform-Mona block on North America plate
Present-day position of Cuba
North America plate (~20 mm/yr)
Mid-Cayman spreading center
SE end of subducted Bahama Platform (Mona block)
A. Earliest Miocene (23.7 Ma)
Reconstructed positions of Cuba, Bahama Platform-Mona block on North America plate
SE end of subducted Bahama Platform (Mona block)
North America plate (~20 mm/yr)
Undisturbed pelagic basin, southern Hispaniola
Initial rifting in Anegada Passage
B. Late Miocene (11.2 Ma)
Reconstructed positions of Cuba, Bahama Platform-Mona block on North America plate
Mona block
Collapse of the northern shelf of Puerto Rico in the wake of the subducted Bahama Platform
North America plate (~18-20 mm/yr)
Topographic uplift and SW-directed folding and thrusting of Hispaniola
Early phase of Mona rifting
C. Late Pliocene (3.4 Ma)
North America plate (~18-20 mm/yr)
Easternmost extent of subducted Bahama Platform (Mona block)
GPS site
2
3
1
"Rigid" area of Caribbean plate at rates 1.5 mm/yr
Active thrust area of Muertos trench
Mona rift zone
Inactive thrust area of Muertos trench
D. Present

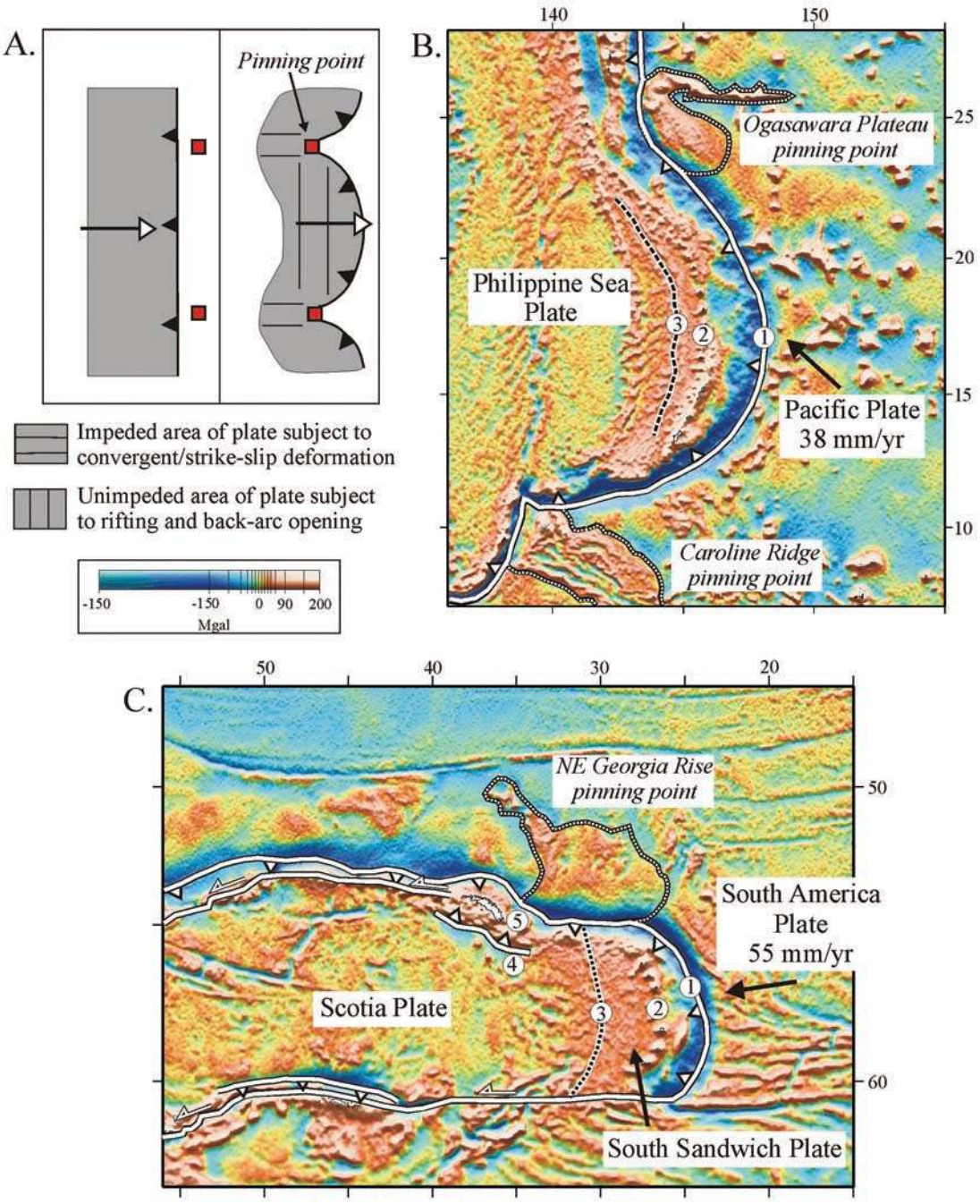

Figure 10. (a) Conceptual model for deformation of an arc by pinning at thicker than normal ridges on oceanic crust (red squares) (modified from *Marshak* [1988]). (b) Pinning of the Marianas arc at its northern and southern ends by the Ogasawara Plateau and the Caroline Ridge. Base map is a satellite-derived gravity map of the Caribbean compiled by *Sandwell and Smith* [1997]. Key to numbered features: 1 = Marianas trench; 2 = Marianas volcanic arc; 3 = Marianas back arc basin. (c) Pinning of the Scotia plate by oblique subduction of the Northeast Georgia Rise, a large igneous province on the seafloor of the South Atlantic Ocean. Key to numbered features: 1 = South Sandwich trench; 2 = South Sandwich arc; 3 = East Scotia back arc basin; 4 = possible backthrust southwest of South Georgia Island; 5 = South Georgia Island. See text for discussion.